Hindawi
Computational and Mathematical Methods in Medicine
Volume 2017, Article ID 1473287, 29 pages
https://doi.org/10.1155/2017/1473287

Research Article

A Multiscale Model for the World's First Parasitic Disease Targeted for Eradication: Guinea Worm Disease

Rendani Netshikweta and Winston Garira

Modelling Health and Environmental Linkages Research Group (MHELRG), Department of Mathematics and Applied Mathematics, University of Venda, Private Bag X5050, Thohoyandou 0950, South Africa

Correspondence should be addressed to Winston Garira; winston.garira@univen.ac.za

Received 13 October 2016; Revised 8 April 2017; Accepted 15 May 2017; Published 20 July 2017

Academic Editor: José Siri

Guinea worm disease (GWD) is both a neglected tropical disease and an environmentally driven infectious disease. Environmentally driven infectious diseases remain one of the biggest health threats for human welfare in developing countries and the threat is increased by the looming danger of climate change. In this paper we present a multiscale model of GWD that integrates the within-host scale and the between-host scale. The model is used to concurrently examine the interactions between the three organisms that are implicated in natural cases of GWD transmission, the copepod vector, the human host, and the protozoan worm parasite *(Dracunculus medinensis)*, and identify their epidemiological roles. The results of the study (through sensitivity analysis of R_0) show that the most efficient elimination strategy for GWD at between-host scale is to give highest priority to copepod vector control by killing the copepods in drinking water (the intermediate host) by applying chemical treatments (e.g., temephos, an organophosphate). This strategy should be complemented by health education to ensure that greater numbers of individuals and communities adopt behavioural practices such as voluntary reporting of GWD cases, prevention of GWD patients from entering drinking water bodies, regular use of water from safe water sources, and, in the absence of such water sources, filtering or boiling water before drinking. Taking into account the fact that there is no drug or vaccine for GWD (interventions which operate at within-host scale), the results of our study show that the development of a drug that kills female worms at within-host scale would have the highest impact at this scale domain with possible population level benefits that include prevention of morbidity and prevention of transmission.

1. Introduction

Guinea worm disease (GWD), sometimes known as *Dracunculiasis* or dracontiasis [1], is a nematode infection transmitted to humans exclusively through contaminated drinking water. People become infected when they drink water contaminated with copepods or cyclopoids (tiny aquatic crustaceans) harbouring infective Dracunculus larvae also known as *Dracunculus medinensis*. The larvae of *Dracunculus medinensis* are released into the stomach, when the copepods are digested by the effect of the gastric juice and get killed by the acid environment. Although the disease has low mortality, its morbidity is considerably high causing huge economic losses and devastating disabilities [2]. There is no vaccine or drug for the disease. Our ability to eliminate GWD rests partly on gaining better insights into the functioning of the immune system, especially its interaction with Guinea worm parasite and partly on development of drugs to treat the disease together with implementation of preventive measures. Currently, the only therapy for GWD is to physically extract the worm from the human body. Humans are the sole definitive host for GWD parasite. Efforts to eradicate the disease are focused on preventive measures which include the following:

(a) *Parasite control in the physical water environment*. This may involve chlorination of drinking water, or boiling the water before drinking, or applying a larvicide, all of which have the effect of killing the parasite and thereby reduce parasite population in the physical water environment.

(b) *Parasite control within the human host*. This involves physically extracting the worm from the human body

by rolling it over an ordinary stick or matchstick [1, 3] and ensuring that the patient receives care by cleaning and bandaging the wound until all the worms are extracted from the patient. This process may take up to two months to complete, as the worm can grow up to a meter in length and only 1-2 centimeters can be removed per day [4, 5].

(c) *Vector control*. This consists of killing the copepods in water (the intermediate host) by applying a chemical called temephos, an organophosphate, to unsafe drinking water sources every month during the transmission season, thus reducing vector population and reducing the chances of individuals contracting the disease [2, 6, 7]. The adult vector may also be removed from drinking water by filtering the water using a nylon cloth or by boiling the water.

(d) *Health education*. This is disseminated through poster, radio and television broadcast, village criers and markets, face-to-face communication (social mobilization and house-to-house visits) by health workers and volunteers to ensure that greater numbers of individuals and communities adopt behavioural practices aimed at preventing transmission of GWD [8]. These behavioural practices include voluntary reporting of GWD cases, prevention of GWD patients from entering drinking water bodies, regular use of water from safe water sources, and, in the absence of such water sources, filtering or boiling water before drinking [6].

(e) *Provision of safe water sources*. This involves providing safe drinking water supplies through protecting hand-dug wells and sinking deep bore wells, improving existing surface water sources by constructing barriers to prevent humans from entering water, and filtering the water through sand-filters [4].

To date, these preventive measures have reduced the incidence of GWD by over 99% [6], making GWD the most likely parasitic disease that will soon be eradicated without the use of any drug or vaccine. Most countries, including the whole of Asia, are now declared free from GWD and transmission of the disease is now limited to African countries, especially Sudan, Ghana, Mali, Niger, and Nigeria [8]. GWD is one of the neglected tropical diseases. It is also an environmentally driven infectious disease. Therefore, its transmission depends on the parasite's survival in the environment and finding new hosts (humans and copepod vectors) in order to replicate and sustain parasite population. Because this process is complex, it has hampered eradication efforts. During the parasite's movement through the environment to the human and copepod vector hosts, many environmental factors influence both the parasite's population and the vector population.

For infectious diseases, including environmentally driven infectious diseases such as GWD, mathematical models have a long history of being used to study their transmission and also to compare and evaluate the effectiveness and affordability of intervention strategies that can be used to control or eliminate them [9, 10]. Currently, the predominant focus of modelling of infectious diseases is centered on concepts of epidemiological modelling and immunological modelling being considered as separate disease processes even for the same infectious disease. In epidemiological or between-host modelling of infectious diseases, the focus is on studying of transmission of infectious diseases between hosts, be they animals or humans or even both in the case of multiple host infections. In the immunological or within-host modelling of infectious diseases, the focus is on studying the interaction of pathogen and the immune system together with other within-host processes in order to elucidate outcomes of infection within a single host [11, 12]. To the best of our knowledge there has been no mathematical model to study the multiscale nature of GWD transmission by integrating between-host scale and within-host scale disease processes. Such models are sometimes called immunoepidemiological models [13]. Most of the mathematical models that have been developed so far are focused on the study of GWD at the epidemiological scale [14–16]. The purpose of this study is to develop an immunoepidemiological model of GWD. Immunoepidemiological modelling of infectious diseases is the quantitative approach which assists in developing a systems approach to understanding infectious disease transmission dynamics with regard to the interdependences between epidemiological (between-host scale) and immunological (within-host scale) processes [17, 18]. The immunoepidemiological model of GWD presented in this paper is based on a modelling framework of the immunoepidemiology of environmentally driven infectious diseases developed recently by the authors [13]. This new and innovative immunoepidemiological modelling framework, while maintaining the limits of a mathematical model, offers a solid platform to bring the separate modelling efforts (immunological modelling and epidemiological modelling) that focus on different aspects of the disease processes together to cover a broad range of disease aspects and time-scales in an integrated systems approach. It bridges host, environmental, and parasitic disease phenomena using mathematical modelling of parasite-host-environment-vector interactions and epidemiology to illuminate the fundamental processes of disease transmission in changing environments. For GWD there are three distinct time-scales associated with its transmission cycle which are as follows.

(i) *The epidemiological time-scale*, which is associated with the infection between hosts (human and copepod vector hosts).

(ii) *The within-host time-scale*, which is related to the replication and developmental stages of Guinea worm parasite within an individual human host and the individual copepod vector host.

(iii) *The environmental time-scale*, which is associated with the abundance and survival of Guinea worm parasite population and vector population in the physical water environment.

In order to try and integrate these different processes and the associated time-scales of GWD, the immunoepidemiological model of GWD presented here incorporates the actual parasite load of the human host and copepod vector, rather

than simply tracking the total number of infected humans. It also incorporates the various stages of the parasite's life cycle as well as the within-host effects such as the effect of gastric juice within an infected human host and describes how the life stages in the definitive human host, environment, and intermediate vector are interconnected with the parasite's life cycle through contact, establishment, and parasite fecundity. The paper is organized as follows. In Section 2 we present brief discussion of the life cycle of Guinea worm parasite and use this information to develop the immunoepidemiological model of GWD in the same section. In Sections 3, 4, and 5, we derive the analytical results associated with the immunoepidemiological model and show that the model is mathematically and epidemiologically well-posed. We also show the reciprocal influence between the within-host scale and between-host scale of GWD transmission dynamics. The results of the sensitivity analysis of the reproductive number are given in Section 6 while the numerical results of the model are presented in Section 7. The paper ends with conclusions in Section 8.

2. The Mathematical Model

We develop a multiscale model of Guinea worm disease that traces the parasite's life cycle of Guinea worm disease. The life cycle of GWD involves three different environments: physical water environment, biological human host environment, and biological copepod host environment. For more details on the life cycle of GWD see the published works [6, 19]. We only give a brief description in this section. The transmission cycle of Guinea worm disease begins when the human individual drinks contaminated water with copepods that are infected with Guinea mature worm larvae (L3 larvae). After ingestion, gastric juice in the human stomach kills the infected copepods and mature worm larvae are released. Then the released mature worm larvae penetrate the human stomach and intestinal wall and move to abdominal tissues where they grow and mate. After mating the male worms die soon and fertilized female worms migrate towards the skin surface (usually on the lower limbs or feet). After a year of infection, the fertilized female worm makes a blister on the infected individual's skin causing burning and itching, which forces an infected individual to immerse his or her feet into water (which is the only source of drinking water) to seek relief from pain. At that point the female worm emerges and releases thousands of worm eggs. The worm eggs then hatch Guinea worm larvae (L1 larvae stage) which are then consumed by copepods and take approximately two weeks to develop and become infective mature larvae (L3 larvae) within the copepods. Then ingestion of the infected copepods by human closes the life cycle. The multiscale model which we now present explicitly traces this life cycle of *Dracunculus medinensis* in three different environments, which are physical water environment, biological human environment, and biological copepod environment. The model flow diagram is shown in Figure 1.

The full multiscale model presented in this paper is based on monitoring the dynamics of ten populations at any time t, which are susceptible humans $S_H(t)$ and infected humans $I_H(t)$ in the behavioural human environment; infected copepods I_C in the human biological environment; mature Guinea worms $W_M(t)$ and fertilized female Guinea worms $W_F(t)$ in the biological human environment (within-host parasite dynamics); Guinea worm eggs $E_W(t)$ and Guinea worm larvae $L_W(t)$ in the physical water environment; susceptible copepods $S_E(t)$ and infected copepods $I_E(t)$ in the physical water environment; and gastric juice $G_J(t)$ in the human biological environment. We make the following assumptions for the model:

(a) There is no vertical transmission of the disease.

(b) The transmission of the disease in the human population is only through drinking contaminated water with infected copepods, $I_E(t)$, harbouring infective free-living pathogens (first-stage larvae), $L_W(t)$, in the physical water environment.

(c) For an infected individual, more than one Guinea worm can emerge simultaneously or sequentially over the course of weeks, depending on the number and intensity of infection the preceding year.

(d) Humans do not develop temporary or permanent immunity.

(e) Copepods do not recover from infection.

(f) The total population of humans and copepods is constant.

(g) Except for the effects of gastric juice in the stomach, there is no immune response in the human host.

(h) Copepods die in the human stomach due to the effects of gastric juice at a rate α_C before their larvae undergoes two molts in the copepod to become L3 larvae and therefore are nonviable and noninfectious larvae.

From the model flow diagram presented in Figure 1 and the assumptions that we have now made, we have the following system of ordinary differential equations as our multiscale model for GWD transmission dynamics:

$$(1)\quad \frac{dS_H(t)}{dt} = \Lambda_H - \lambda_H(t) S_H(t) - \mu_H S_H(t) + \alpha_H I_H(t),$$

$$(2)\quad \frac{dI_H(t)}{dt} = \lambda_H(t) S_H(t) - (\mu_H + \delta_H + \alpha_H) I_H(t),$$

$$(3)\quad \frac{dI_C(t)}{dt} = \lambda_h(t) S_h(t) - \mu_C G_J(t) I_C(t) - \alpha_C I_C(t),$$

$$(4)\quad \frac{dW_M(t)}{dt} = N_C \mu_C G_J(t) I_C(t) - (\alpha_M + \mu_M) W_M(t),$$

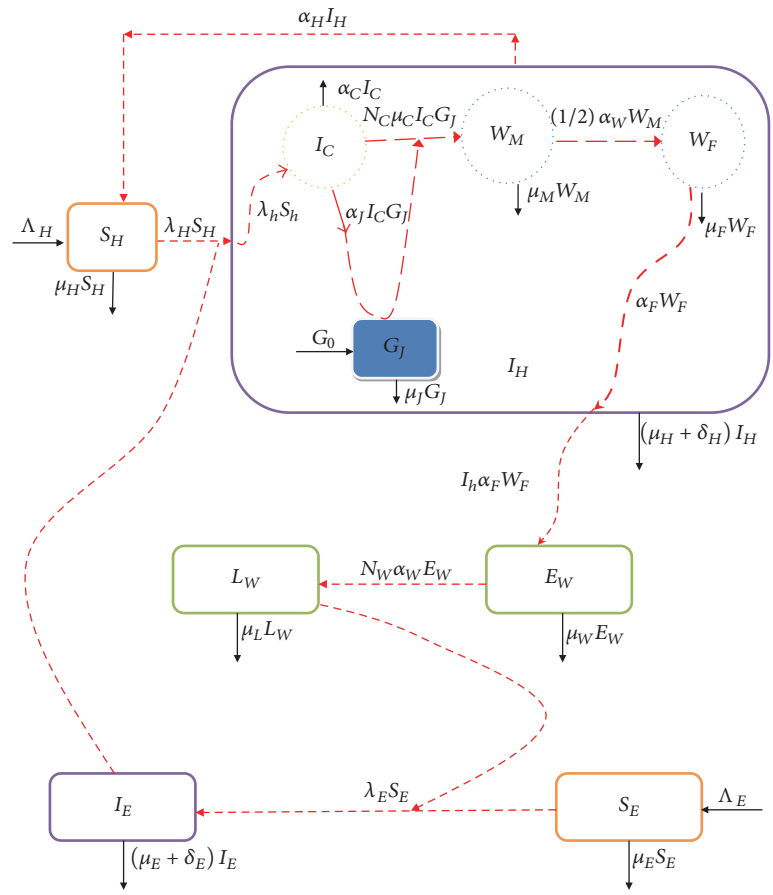

Figure 1: A conceptual diagram of the multiscale model of Guinea worm disease transmission dynamics.

$$
\begin{aligned}
(5)\quad & \frac{dW_F(t)}{dt} = \frac{\alpha_M}{2} W_M(t) - (\mu_F + \alpha_F) W_F(t), \\
(6)\quad & \frac{dG_J(t)}{dt} = G_0 + \alpha_J G_J(t) I_C(t) - \mu_J G_J(t), \\
(7)\quad & \frac{dE_W(t)}{dt} = \alpha_F W_F(t) I_h(t) - (\mu_W + \alpha_W) E_W(t), \\
(8)\quad & \frac{dL_W(t)}{dt} = N_W \alpha_W E_W(t) - \mu_L L_W(t), \\
(9)\quad & \frac{dS_E(t)}{dt} = \Lambda_E - \lambda_E(t) S_E(t) - \mu_E S_E(t), \\
(10)\quad & \frac{dI_E(t)}{dt} = \lambda_E(t) S_E(t) - (\mu_E + \delta_E) I_E(t),
\end{aligned}
\tag{1}
$$

where

$$
\begin{aligned}
\lambda_H(t) &= \frac{\beta_H I_E(t)}{P_0 + \epsilon I_E(t)}, \\
\lambda_E(t) &= \frac{\beta_E L_W(t)}{L_0 + \epsilon L_W(t)}, \\
I_h(t) &= I_H(t) + 1, \\
S_h(t) &= S_H(t) - 1, \\
\lambda_h(t) &= \frac{\beta_H I_E(t)}{[P_0 + \epsilon I_E(t)]\,[I_H(t) + 1]}.
\end{aligned}
\tag{2}
$$

Equations (1) and (2) of the model system (1) describe the evolution with time of susceptible and infected human hosts, respectively. At any time t, new susceptible humans are recruited at a constant rate Λ_H and we assume that the recruited humans are all susceptible. Susceptible individuals leave the susceptible class either through infection at rate $\lambda_H(t)S_H(t)$ by drinking contaminated water with infected copepods to join infected group or through natural death at a rate μ_H. The infected group is generated through infection when susceptible humans acquire the disease at a rate $\lambda_H(t)S_H(t)$ through drinking water contaminated with copepods infected with *Dracunculus medinensis*. Infected humans leave the infected group either through recovery at a rate α_H to join the susceptible group or through natural death at a rate μ_H, or through disease induced death at a rate δ_H. Equation (3) of the model system (1) represents the evolution with time of infected copepods within an infected human host. The infected copepods within a human host are generated following uptake of infected copepods in the physical water environment through drinking contaminated

water. In the human population, this uptake of infected copepods, which harbour Guinea worm larvae, is the transmission of Guinea worm parasite from the physical water environment to susceptible humans who become infected humans. Following the methodology described in [13] for modelling reinfection (superinfection) for environmentally transmitted infectious disease systems (because GWD and schistosomiasis are both water-borne and vector-borne infections), we model the average rate at which a single susceptible human host uptakes the infected copepods in the physical water environment through drinking contaminated water and becomes an infected human host by the expression

$$\lambda_h(t) S_h(t) = \frac{\lambda_H(t) \left[S_H(t) - 1\right]}{\left[I_H(t) + 1\right]}, \tag{3}$$

where $\lambda_H(t)$, $S_H(t)$, and $I_H(t)$ are as defined previously. This is because, in our case, we define such a single infection by a single transition

$$\begin{aligned} &\left(S_H(t), I_H(t), I_E(t)\right) \\ &\quad \longrightarrow \left(S_H(t) - 1, I_H(t) + 1, I_E(t)\right). \end{aligned} \tag{4}$$

Therefore, the average number of infected copepods, $I_C(t)$, within a single infected human host increases at a mean rate $\lambda_h(t)S_h(t)$ and decreases through death due to digestion by human gastric acid at a rate μ_C after their larvae undergo two molts in the copepod to become L3 larvae and release viable and infectious larvae or naturally at a rate α_C before their larvae undergo two molts in the copepod to become L3 larvae and release nonviable and noninfectious larvae.

Equations (4–6) of the model system (1) represent changes with time of the average population of mature worms $W_M(t)$, fertilized female worms $W_F(t)$, and the amount of gastric acid $G_J(t)$ within a single infected human host, respectively. The average mature worm population $W_M(t)$ in a single infected human host is generated following the digestion of infected copepods in the human stomach by gastric acid and then mature worms are released. We assume that mature worms die naturally at a rate μ_M and they exit the human stomach to the abdominal tissues at a rate α_M, where they grow and mate. The population of fertilized female worms, $W_F(t)$ within an infected human host, is generated following the developmental changes undergone by mature fertilized female worms. These developmental changes result in mature worms reaching sexual maturity and mating and all male worms die soon after mating. We assume that fertilized female worms die naturally at a rate μ_F and emerge out through an infected human individual's skin (usually the lower limbs) to release Guinea worm eggs into a water source at a rate α_F, when an infected human comes into contact with water. The average amount of gastric acid inside a human stomach is generated following copepod vector induced proliferation at a rate $\alpha_J I_C(t)$, which is proportional to the density of infected copepods within an infected human host. We assume that the amount of gastric acid is also increased by the spontaneous production of gastric acid by the human body at a rate G_0 and diluted or degraded at a rate μ_J. Equation (7) of model system (1) describes the evolution with time of the Guinea worm eggs $E_W(t)$ in the physical water environment. We note that the population of Guinea worm eggs increases when each infected human host excretes eggs at a rate $\alpha_F W_F(t)$. Therefore the rate at which infected humans contaminate the physical water environment by excreting Guinea worm eggs is modelled by $\alpha_F W_F(t) I_h(t)$. The last three equations of the model system (1) describe the evolution with time of Guinea worm larvae $L_W(t)$, susceptible copepods $S_E(t)$, and infected copepods $I_E(t)$ in the physical water environment, respectively. The population of Guinea worm larvae is generated through each egg hatching an average of N_W worms larvae with eggs hatching at an average rate of α_W. Therefore the total Guinea worm larvae in the physical water environment are modelled by $N_W \alpha_W E_W(t)$. We assume that worm larvae in the physical water environment die naturally at a constant rate μ_L. Similar to human population, at any time t, new susceptible copepods are recruited at a constant Λ_E. Susceptible copepods leave the susceptible group to join the infected copepods group through infection at a rate $\lambda_E(t)S_E(t)$ when they consume first-stage Guinea worm larvae in the physical water environment. We assume that the population of copepods die naturally at a constant rate μ_E and further, we also assume that infected copepods have an additional mortality rate δ_E due to infection. The model state variables are summarized in Table 1.

3. Invariant Region of the Model

The model system (1) can be analysed in a region $\Omega \subset \mathbb{R}_+^{10}$ of biological interest. Now assume that all parameters and state variables for model system (1) are positive for all $t > 0$ and further suppose that G_J is bounded above by G_0/μ_J. It can be shown that all solutions for the model system (1) with positive initial conditions remain bounded.

Letting $N_H = S_H + I_H$ and adding (1) and (2) of model system (1) we obtain

$$\begin{aligned} \frac{dS_H}{dt} + \frac{dI_H}{dt} = \frac{dN_H}{dt} &= \Lambda_H - \mu_H N_H - \delta_H I_H \\ &\leq \Lambda_H - \mu_H N_H. \end{aligned} \tag{5}$$

This implies that

$$\lim_{t \to \infty} \sup\left(N_H(t)\right) \leq \frac{\Lambda_H}{\mu_H}. \tag{6}$$

Similarly, letting $N_E = S_E + I_E$ and adding (9) and (10) of model system (1) we obtain

$$\begin{aligned} \frac{dS_E}{dt} + \frac{dI_E}{dt} = \frac{dN_E}{dt} &= \Lambda_E - \mu_H N_E - \delta_H I_E \\ &\leq \Lambda_E - \mu_H N_E. \end{aligned} \tag{7}$$

This also implies that

$$\lim_{t \to \infty} \sup\left(N_E(t)\right) \leq \frac{\Lambda_E}{\mu_E}. \tag{8}$$

Table 1: Description of the state variables of the model system (1).

State variable	Description	Initial value
$S_H(t)$	The susceptible human population size in the behavioural human environment	2500
$I_H(t)$	The infected human population size in the behavioural human environment	10
$I_C(t)$	The infected copepod population size in the biological human environment	0
$W_M(t)$	The mature worm population size in the biological human environment	0
$W_F(t)$	The female worm population size in the biological human environment	0
$G_J(t)$	Amount of gastric acid in the human stomach	1.5
$S_E(t)$	The susceptible copepod population size in the physical water environment	10^5
$I_E(t)$	The infected copepod population size in the physical water environment	0
$E_W(t)$	The worm egg population size in the physical water environment	0
$L_W(t)$	The worm larvae population size in the physical water environment	5000

Now considering the third equation of model system (1), given by

$$\begin{aligned}\frac{dI_C}{dt} &= \lambda_h S_h - \mu_C G_J I_C - \delta_C I_C \\ &= \left(\frac{\beta_H I_E (S_H - 1)}{(P_0 + \epsilon I_E)(I_H + 1)}\right) - (\mu_C G_J + \alpha_C) I_C,\end{aligned} \tag{9}$$

we obtain

$$\begin{aligned}\frac{dI_C}{dt} \le &\left(\frac{\beta_H \Lambda_E (\Lambda_H - \mu_H)}{(P_0\mu_E + \epsilon\Lambda_E)(\Lambda_H + \mu_H)}\right) \\ &- \frac{1}{\mu_J}(\mu_C G_0 + \alpha_C \mu_J) I_C.\end{aligned} \tag{10}$$

This implies that

$$\begin{aligned}&\lim_{t\to\infty} \sup (I_C(t)) \\ &\le \left(\frac{\beta_H \Lambda_E (\Lambda_H - \mu_H)}{(P_0\mu_E + \epsilon\Lambda_E)(\Lambda_H + \mu_H)}\right)\left(\frac{\mu_J}{(\mu_C G_0 + \delta_H \mu_J)}\right).\end{aligned} \tag{11}$$

Using (6), (8), and (11) similar expression can be derived for the remaining model variables. Hence, all feasible solutions of the model system (1) are positive and enter a region defined by

$$\begin{aligned}\Omega = \{&(S_H, I_H, I_C, W_M, W_F, G_J, E_W, L_W, S_E, I_E) \\ &\in \mathbb{R}_+^{10} : 0 \le S_H + I_H \le S_1,\ 0 \le S_E + I_E \le S_2,\ 0 \le I_C \\ &\le S_3,\ 0 \le W_M \le S_4,\ 0 \le W_F \le S_5,\ 0 \le G_J \le S_6,\ 0 \\ &\le E_W \le S_7,\ 0 \le L_W \le S_8\},\end{aligned} \tag{12}$$

which is positively invariant and attracting for all $t > 0$, where

$$\begin{aligned}S_1 &= \frac{\Lambda_H}{\mu_H}, \\ S_2 &= \frac{\Lambda_E}{\mu_E}, \\ S_3 &= \left(\frac{\mu_J}{(\mu_C G_0 + \alpha_C \mu_J)}\right) S_9, \\ S_4 &= \left(\frac{N_C \alpha_C \mu_C}{\alpha_M + \mu_M}\right)\left(\frac{\mu_J}{(\mu_C G_0 + \alpha_C \mu_J)}\right) S_9, \\ S_5 &= \frac{1}{2}\left(\frac{\alpha_M}{\alpha_F + \mu_F}\right)\left(\frac{N_C \alpha_C \mu_C}{\alpha_M + \mu_M}\right)\left(\frac{\mu_J}{(\mu_C G_0 + \alpha_C \mu_J)}\right) S_9, \\ S_6 &= \frac{G_0}{\mu_J}, \\ S_7 &= \frac{1}{2}\left(\frac{\alpha_F}{\alpha_W + \mu_W}\right)\left(\frac{\alpha_M}{\alpha_F + \mu_F}\right)\left(\frac{N_C \alpha_C \mu_C}{\alpha_M + \mu_M}\right) \\ &\quad \cdot \left(\frac{\mu_J}{(\mu_C G_0 + \alpha_C \mu_J)}\right) S_9, \\ S_8 &= \frac{1}{2}\left(\frac{N_W \alpha_W}{\mu_L}\right)\left(\frac{\alpha_F}{\alpha_W + \mu_W}\right)\left(\frac{\alpha_M}{\alpha_F + \mu_F}\right) \\ &\quad \cdot \left(\frac{N_C \alpha_C \mu_C}{\alpha_M + \mu_M}\right)\left(\frac{\mu_J}{(\mu_C G_0 + \alpha_C \mu_J)}\right) S_9, \\ S_9 &= \left(\frac{\beta_H \Lambda_C (\Lambda_H - \mu_H)}{(P_0\mu_C + \epsilon\Lambda_C)(\Lambda_H + \mu_H)}\right).\end{aligned} \tag{13}$$

Therefore it is sufficient to consider solutions of the model system (1) in Ω, since all solutions starting in Ω remain there for all $t \ge 0$. Hence, the model system is mathematically and epidemiologically well-posed and it is sufficient to consider the dynamics of the flow generated by model system (1) in Ω whenever $\Lambda_H > \mu_H$. We shall assume in all that follows (unless stated otherwise) that $\Lambda_H > \mu_H$.

4. Determination of Disease-Free Equilibrium and Its Stability

To obtain the disease-free equilibrium point of system (1), we set the left-hand side of the equations equal to zero and

further we assume that $I_H = I_C = W_H = W_H = E_W = L_W = I_E = 0$. This means that all the populations are free from the disease. Thus we get

$$E_0 = \left(S_H^0, I_H^0, I_C^0, W_M^0, W_F^0, G_J^0, E_W^0, L_W^0, S_E^0, I_E^0\right), = \left(\frac{\Lambda_H}{\mu_H}, 0, 0, 0, 0, \frac{G_0}{\mu_J}, 0, 0, \frac{\Lambda_E}{\mu_E}, 0\right), \tag{14}$$

as the disease-free equilibrium of the model system (1).

4.1. The Basic Reproduction Number of the Model System (1). The basic reproduction number of the system model (1) is calculated in this section using next generation operator approach described in [20]. Thus the model system (1) can also be written in the form

$$\frac{dX}{dt} = f(X, Y, Z), \quad \frac{dY}{dt} = g(X, Y, Z), \quad \frac{dZ}{dt} = h(X, Y, Z), \tag{15}$$

where

(i) $X = (S_H, S_E, G_J)$ represents all compartments of individuals who are not infected,

(ii) $Y = (I_H, I_C, W_M, W_F, E_W)$ represents all compartments of infected individuals who are not capable of infecting others,

(iii) $Z = (I_E, L_W)$ represents all compartments of infected individuals who are capable of infecting others.

We also let the disease-free equilibrium of the model (1) be denoted by the following expression:

$$\overline{U}_0 = \left(\frac{\Lambda_H}{\mu_H}, 0, 0, 0, 0, \frac{G_0}{\mu_J}, 0, 0, \frac{\Lambda_E}{\mu_E}, 0\right). \tag{16}$$

Following [20], we let

$$\widetilde{g}(X^*, Z) = \left(\widetilde{g}_1(X^*, Z), \widetilde{g}_2(X^*, Z), \widetilde{g}_3(X^*, Z), \widetilde{g}_4(X^*, Z), \widetilde{g}_5(X^*, Z)\right), \tag{17}$$

with

$$\begin{aligned}
\widetilde{g}_1(X^*, Z) &= \frac{\beta_H \Lambda_H Z_1}{\mu_H(\mu_H + \delta_H + \alpha_H)(P_0 + \epsilon I_E)},\\
\widetilde{g}_2(X^*, Z) &= \frac{\beta_H(\Lambda_H - \mu_H)\mu_J(\mu_H + \delta_H + \alpha_H)Z_1}{(\mu_C G_0 + \mu_J \alpha_C) M_{11}},\\
\widetilde{g}_3(X^*, Z) &= \frac{N_C \alpha_C \beta_H(\Lambda_H - \mu_H) G_0(\mu_H + \delta_H + \alpha_H) Z_1}{(\mu_M + \alpha_M)(\mu_C G_0 + \mu_J \alpha_C) M_{11}},\\
\widetilde{g}_4(X^*, Z) &= \frac{\alpha_M N_C \alpha_C \beta_H(\Lambda_H - \mu_H) G_0(\mu_H + \delta_H + \alpha_H) Z_1}{2(\mu_F + \alpha_F)(\mu_M + \alpha_M)(\mu_C G_0 + \mu_J \alpha_C) M_{11}},\\
\widetilde{g}_5(X^*, Z) &= \frac{\alpha_F \alpha_M N_C \alpha_C \beta_H(\Lambda_H - \mu_H) G_0 Z_1}{2(\mu_W + \alpha_W)(\mu_F + \alpha_F)(\mu_M + \alpha_M)(\mu_C G_0 + \mu_J \alpha_C)\mu_H(P_0 + \epsilon I_E)},
\end{aligned} \tag{18}$$

where

$$M_{11} = \epsilon \beta_H \Lambda_H I_E + \mu_H(\mu_H + \delta_H + \mu_H)(P_0 + \epsilon I_E). \tag{19}$$

We deduce that

$$h(X, Y, Z) = \left(h_1(X, Y, Z), h_2(X, Y, Z)\right), \tag{20}$$

with

$$\begin{aligned}
h_1(X, Y, Z) &= \lambda_E S_E - (\mu_E + \alpha_E) I_E\\
&= \frac{\beta_E \Lambda_E Z_2}{\mu_E(L_0 + \epsilon Z_2)} - (\mu_E + \alpha_E) Z_1,\\
h_2(X, Y, Z) &= N_W \alpha_W E_W - \mu_L L_W\\
&= \frac{K Z_1}{(P_0 + \epsilon Z_1)} - \mu_L Z_2,
\end{aligned} \tag{21}$$

where

$$K = \frac{\alpha_F \alpha_M N_W \alpha_W N_C \alpha_C \beta_H (\Lambda_H - \mu_H) G_0}{2(\mu_W + \alpha_W)(\mu_F + \alpha_F)(\mu_M + \alpha_M)(\mu_C G_0 + \mu_J \alpha_C)\mu_H}. \quad (22)$$

A matrix

$$A = D_Z h(X^*, \tilde{g}(X^*, 0), 0) = \begin{bmatrix} -(\mu_E + \alpha_E) & \frac{K}{P_0} \\ \frac{\beta_E \Lambda_E}{\mu_E L_0} & -\mu_L \end{bmatrix} \quad (23)$$

can be written in the form $A = M - D$, so that

$$M = \begin{bmatrix} 0 & \frac{K}{P_0} \\ \frac{\beta_E \Lambda_E}{\mu_E L_0} & 0 \end{bmatrix}, \quad (24)$$

$$D = \begin{bmatrix} (\mu_E + \alpha_E) & 0 \\ 0 & \mu_L \end{bmatrix}. \quad (25)$$

The basic reproductive number is the spectral radius (dominant eigenvalue) of the matrix $T = MD^{-1}$. Hence, the basic reproduction number of the immumoepidemiological model (1) is expressed by the following quantity.

$$R_0 = \sqrt{\frac{1}{2} \cdot \frac{\alpha_M}{\alpha_M + \mu_M} \cdot \frac{\alpha_F}{\alpha_F + \mu_F} \cdot \frac{N_C \mu_C G_0}{\mu_C G_0 + \mu_J \alpha_C} \cdot \frac{\beta_H (\Lambda_H - \mu_H)}{P_0 \mu_H} \cdot \frac{N_W \alpha_W}{(\alpha_W + \mu_W)\mu_L} \frac{\beta_E \Lambda_E}{\mu_E (\mu_E + \delta_E) L_0}}$$
$$= \sqrt{R_{0B} R_{0W}}, \quad (26)$$

with

$$R_{0B} = \frac{\beta_H (\Lambda_H - \mu_H)}{P_0 \mu_H} \cdot \frac{N_W \alpha_W}{(\alpha_W + \mu_W)\mu_L} \frac{\beta_E \Lambda_E}{\mu_E (\mu_E + \delta_E) L_0}, \quad (27)$$

$$R_{0W} = \frac{1}{2} \cdot \frac{\alpha_M}{\alpha_M + \mu_M} \cdot \frac{\alpha_F}{\alpha_F + \mu_F} \cdot \frac{N_C \mu_C G_0}{\mu_C G_0 + \mu_J \alpha_C}. \quad (28)$$

The expression, R_{0B}, in (27) represents GWD's partial reproductive number associated with the between-host transmission of the disease while the expression, R_{0W}, in (28) represents GWD's partial reproductive number associated with the within-host transmission of the disease. From the above two expressions in (27) and (28), respectively, we therefore make the following deductions.

(i) The epidemiological (between-host) transmission parameters such as the rate at which susceptible humans come into contact with water contaminated with infected copepods β_H (through drinking contaminated water with infected copepods) and the rate at which susceptible copepods come into contact with Guinea worm larvae β_E; the supply rate of susceptible humans Λ_H and copepods Λ_E (through birth); the rate at which worms emerge from infected humans to contaminate the physical water environment α_F, by laying eggs every time infected humans come into contact with water sources; the rate at which eggs in physical water environment hatch to produce worm larvae $N_W \alpha_W$ all contribute to the transmission of Guinea worm disease. Therefore control measures such as reducing the rate at which infected human hosts visit water sources when an individual is infected, reducing contact rate between susceptible humans with contaminated water through educating the public, and treating water bodies with chemicals that kill worm eggs, worm larvae, and copepods may help to reduce the transmission risk of GWD.

(ii) The immunological (within-host) transmission parameters such as the rate at which infected copepods within an infected human host release mature worms $N_C \mu_C$ after digestion by human gastric juice; the rate at which mature worms become fertilized females worms $\alpha_M/2$; and the rate at which mature worms and females worms die all contribute to the transmission of Guinea worm disease. Therefore immune mechanisms that kill infected copepods and worms within infected human host and also treatment intend to kill both mature worms and fertilized female worm population may help to reduce the transmission risk of GWD.

Therefore, both the epidemiological and immunological factors affect the transmission cycle of GWD in both humans and copepod population.

4.2. Local Stability of DFE. In this section we determine the local stability of DFE of the model system (1). We linearize equations of the model system (1) in order to obtain a Jacobian matrix. Then we evaluate the Jacobian matrix of the system at the disease-free equilibrium (DFE),

$$E_0 = \left(\frac{\Lambda_H}{\mu_H}, 0, 0, 0, 0, \frac{G_0}{\mu_J}, 0, 0, \frac{\Lambda_E}{\mu_E}, 0 \right). \quad (29)$$

The Jacobian matrix of the model system (1) evaluated at the disease-free equilibrium state (DFE) is given by

$$J(E_0) = \begin{pmatrix} -\mu_H & \alpha_H & 0 & 0 & 0 & 0 & 0 & 0 & 0 & -A_0 \\ 0 & -q_0 & 0 & 0 & 0 & 0 & 0 & 0 & 0 & A_0 \\ 0 & 0 & -q_1 & 0 & 0 & 0 & 0 & 0 & 0 & A_1 \\ 0 & 0 & \dfrac{N_C\mu_C G_0}{\mu_J} & -q_2 & 0 & 0 & 0 & 0 & 0 & 0 \\ 0 & 0 & 0 & \dfrac{\alpha_M}{2} & -q_3 & 0 & 0 & 0 & 0 & 0 \\ 0 & 0 & \alpha_J \dfrac{G_0}{\mu_J} & 0 & 0 & -\mu_J & 0 & 0 & 0 & 0 \\ 0 & 0 & 0 & 0 & \alpha_F & 0 & -q_4 & 0 & 0 & 0 \\ 0 & 0 & 0 & 0 & 0 & 0 & N_W\alpha_W & -\mu_L & 0 & 0 \\ 0 & 0 & 0 & 0 & 0 & 0 & 0 & -\dfrac{\beta_E\Lambda_E}{\mu_E L_0} & -\mu_E & 0 \\ 0 & 0 & 0 & 0 & 0 & 0 & 0 & \dfrac{\beta_E\Lambda_E}{\mu_E L_0} & 0 & -q_5 \end{pmatrix}, \tag{30}$$

where

$$\begin{aligned} q_0 &= (\mu_H + \delta_H + \alpha_H), \\ q_1 &= \frac{(\mu_C G_0 + \mu_J \alpha_C)}{\mu_J}, \\ q_2 &= (\mu_M + \alpha_M), \\ q_3 &= (\mu_F + \alpha_F), \\ q_4 &= (\mu_W + \alpha_W), \\ q_5 &= (\mu_E + \alpha_E), \\ A_0 &= \frac{\beta_H \Lambda_H}{P_0 \mu_H}, \\ A_1 &= \frac{\beta_H (\Lambda_H - \mu_H)}{\mu_H P_0}. \end{aligned} \tag{31}$$

We consider stability of DFE by calculating the eigenvalues (λ_s) of the Jacobian matrix given by (30). The characteristic equation for the eigenvalues is given by

$$\begin{aligned} &\lambda_0 \left[\lambda^6 + \pi_1\lambda^5 + \pi_2\lambda^4 + \pi_3\lambda^3 + \pi_4\lambda^2 + \pi_5\lambda + \pi_6\right] \\ &\quad = 0, \end{aligned} \tag{32}$$

where

$$\lambda_0 = (-\mu_H - \lambda)(-\mu_E - \lambda)(-\mu_J - \lambda)(-q_0 - \lambda). \tag{33}$$

It is clear from (32) that there are four negative eigenvalues ($-\mu_H$, $-\mu_E$, $-\mu_J$, and $-q_0$). Now in order to make conclusions about the stability of the DFE, we use the Routh-Hurwitz criteria to determine the sign of the remaining eigenvalues of the polynomial

$$\lambda^6 + \pi_1\lambda^5 + \pi_2\lambda^4 + \pi_3\lambda^3 + \pi_4\lambda^2 + \pi_5\lambda + \pi_6 = 0, \tag{34}$$

where

$$\begin{aligned} \pi_1 &= q_1 + q_2 + q_3 + q_4 + q_5 + \mu_L, \\ \pi_2 &= q_1q_2 + q_3q_4 + (q_1 + q_2 + q_3 + q_4)(q_5 + \mu_L) \\ &\quad + q_5\mu_L + (q_1 + q_2)(q_3 + q_4), \\ \pi_3 &= q_1q_2(q_3 + q_4) + q_3q_4(q_1 + q_2) \\ &\quad + (q_1 + q_2)(q_3 + q_4)(q_5 + \mu_L) \\ &\quad + q_1q_2(q_5 + \mu_L) + q_3q_4(q_5 + \mu_L) \\ &\quad + q_5\mu_L(q_1 + q_2 + q_3 + q_4), \\ \pi_4 &= q_1q_2q_3q_4 + q_3q_4(q_1 + q_2)(q_5 + \mu_L) \\ &\quad + q_1q_2(q_3 + q_4)(q_5 + \mu_L) \\ &\quad + (q_1 + q_2)(q_3 + q_4)q_1\mu_L + q_5q_4q_3\mu_L \\ &\quad + q_1q_2q_5\mu_L, \\ \pi_5 &= q_1q_2q_3q_4(q_5 + \mu_L) + q_3q_4(q_1 + q_2)q_5\mu_L \\ &\quad + q_1q_2(q_3 + q_4)q_5\mu_L, \\ \pi_6 &= q_1q_2q_3q_4q_5\mu_L(1 - R_0^2). \end{aligned} \tag{35}$$

Using the Routh-Hurwitz stability criterion, the equilibrium state associated with the model system (1) is stable if and only if the determinants of all the Hurwitz matrices associated with the characteristic equation (34) are positive; that is,

$$\mathrm{Det}\left(H_j\right) > 0; \quad j = 1, 2, \ldots, 6, \tag{36}$$

where

$$H_1 = (\pi_1);$$

$$H_2 = \begin{pmatrix} \pi_1 & 1 \\ \pi_3 & \pi_2 \end{pmatrix};$$

$$H_3 = \begin{pmatrix} \pi_1 & 1 & 0 \\ \pi_3 & \pi_2 & \pi_1 \\ \pi_5 & \pi_4 & \pi_3 \end{pmatrix};$$

$$H_4 = \begin{pmatrix} \pi_1 & 1 & 0 & 0 \\ \pi_3 & \pi_2 & \pi_1 & 1 \\ \pi_5 & \pi_4 & \pi_3 & \pi_2 \\ 0 & \pi_6 & \pi_5 & \pi_4 \end{pmatrix};$$

$$H_5 = \begin{pmatrix} \pi_1 & 1 & 0 & 0 & 0 \\ \pi_3 & \pi_2 & \pi_1 & 1 & 0 \\ \pi_5 & \pi_4 & \pi_3 & \pi_2 & \pi_1 \\ 0 & \pi_6 & \pi_5 & \pi_4 & \pi_3 \\ 0 & 0 & 0 & \pi_6 & \pi_5 \end{pmatrix};$$

$$H_6 = \begin{pmatrix} \pi_1 & 1 & 0 & 0 & 0 & 0 \\ \pi_3 & \pi_2 & \pi_1 & 1 & 0 & 0 \\ \pi_5 & \pi_4 & \pi_3 & \pi_2 & \pi_1 & 1 \\ 0 & \pi_6 & \pi_5 & \pi_4 & \pi_3 & \pi_2 \\ 0 & 0 & 0 & \pi_6 & \pi_5 & \pi_4 \\ 0 & 0 & 0 & 0 & 0 & \pi_6 \end{pmatrix}. \tag{37}$$

The Routh-Hurwitz criterion applied to (37) requires that the following conditions (H1)–(H6) be satisfied, in order to guarantee the local stability of the disease-free equilibrium point of the model system (1).

(H1) $\pi_1 > 0$.

(H2) $\pi_1\pi_2 - \pi_3 > 0$.

(H3) $\pi_1(\pi_2\pi_3 + \pi_5) > \pi_1\pi_4 + \pi_3^2$.

(H4) $\pi_1[\pi_2(\pi_3(\pi_4 + \pi_5) + \pi_1\pi_6) + (\pi_1 + \pi_4)] > \pi_1[\pi_2^2\pi_5 + \pi_3\pi_6 + \pi_1\pi_4^2] + \pi_3{}^2\pi_4 + \pi_5^2$.

(H5) $\pi_6[\pi_1(2\pi_2\pi_5 + \pi_3(\pi_1\pi_4 - 3\pi_5 - \pi_3)) + \pi_3^3\pi_6] + \pi_5[\pi_5(2\pi_1\pi_4 + \pi_2\pi_3 - \pi_1\pi_2(\pi_2 + 1) + \pi_4(\pi_1\pi_2\pi_3 - \pi_1^2\pi_4 - \pi_3^2))] > 0$.

(H6) $\pi_6^2[\pi_1(2\pi_2\pi_5 + \pi_3(\pi_1\pi_4 - 3\pi_5 - \pi_3)) + \pi_3^3\pi_6] + \pi_5\pi_6[\pi_5(2\pi_1\pi_4 + \pi_2\pi_3 - \pi_1\pi_2(\pi_2 + 1) + \pi_4(\pi_1\pi_2\pi_3 - \pi_1^2\pi_4 - \pi_3^2))] > 0$.

From (37) we note that all the coefficients π_1, π_2, π_3, π_4, π_5, and π_6 of the polynomial $P(\lambda)$ are greater than zero whenever $R_0^2 < 1$. And we also noted that the conditions above are satisfied if and only if $R_0^2 < 1$. Hence all the roots of the polynomial $P(\lambda)$ either are negative or have negative real parts. The results are summarized in the following theorem.

Theorem 1. *The disease-free equilibrium point of the model system (1) is locally asymptotically stable whenever $R_0 < 1$.*

4.3. Global Stability of DFE. To determine the global stability of DFE of the model system (1), we use Theorem 2 in [21] to establish that the disease-free equilibrium is globally asymptotically stable whenever $R_0 < 1$ and unstable when $R_0 > 1$. In this section, we list two conditions that if met, also guarantee the global asymptotic stability of the disease-free state. We write the model system (1) in the form

$$\frac{dX}{dt} = F(X, Z),$$
$$\frac{dY}{dt} = G(X, Z), \tag{38}$$

where

(i) $X = (S_H, S_E, G_J)$ represents all uninfected components.

(ii) $Z = (I_H, I_C, W_M, W_F, E_W, L_W, I_E)$ represents all compartments of infected and infectious components.

We let

$$U_0 = (X^*, 0) = \left(\frac{\Lambda_H}{\mu_H}, 0, 0, \frac{\Lambda_C}{\mu_C}, 0, 0, 0\right) \tag{39}$$

denote the disease-free equilibrium (DFE) of the system. To guarantee global asymptotic stability of the disease-free equilibrium, conditions (H1) and (H2) below must be met [20].

(H1) $dX/dt = F(X, 0)$ is globally asymptotically stable,

(H2) $G(X, Z) = AZ - \widehat{G}(X, Z)$ and $\widehat{G}(X, Z) \geq 0$ for $(X, Z) \in \mathbb{R}_+^{10}$, where $A = D_Z G(X^*, 0)$ is an M-matrix and $\mathbb{R}_+^{10}$ is the region where the model makes biological sense.

In our case

$$F(X, 0) = \begin{bmatrix} \Lambda_H - \mu_H S_H \\ \Lambda_E - \mu_E S_E \\ G_0 - \mu_J G_J \end{bmatrix}. \tag{40}$$

Matrix A is given by

$$A = \begin{bmatrix} -a_0 & 0 & 0 & 0 & 0 & 0 & \frac{\beta_H \Lambda_H}{P_0 \mu_H} \\ 0 & -a_1 & 0 & 0 & 0 & 0 & \frac{\beta_H (\Lambda_H - \mu_H)}{\mu_H P_0} \\ 0 & N_C \mu_C \frac{G_0}{\mu_J} & -a_2 & 0 & 0 & 0 & 0 \\ 0 & 0 & \frac{\alpha_M}{2} & -a_3 & 0 & 0 & 0 \\ 0 & 0 & 0 & \alpha_F & -a_4 & 0 & 0 \\ 0 & 0 & 0 & 0 & N_W \alpha_W & -\mu_L & 0 \\ 0 & 0 & 0 & 0 & 0 & \frac{\beta_E \Lambda_E}{L_0 \mu_E} & -a_5 \end{bmatrix}, \tag{41}$$

where

$$\begin{aligned} a_0 &= (\mu_H + \delta_H + \alpha_H), \\ a_1 &= \frac{1}{\mu_J} (\mu_C + \alpha_C \mu_J), \\ a_2 &= (\mu_M + \alpha_M), \\ a_3 &= (\mu_F + \alpha_F), \\ a_4 &= (\mu_W + \alpha_W), \\ a_5 &= (\mu_E + \alpha_E), \end{aligned}$$

$$\widehat{G}(X, Z) = \begin{bmatrix} \left(\frac{\Lambda_H}{\mu_H P_0} - \frac{S_H}{P_0 + \epsilon I_E} \right) \beta_H I_E \\ \left(\frac{(\Lambda_H - \mu_H)}{\mu_H P_0} - \frac{(S_H - 1)}{P_0 + \epsilon I_E} \right) \beta_H I_E + I_C \left(\mu_C \left(G_J - \frac{G_0}{\mu_J} \right) + \alpha_C (1 - \mu_J) \right) \\ 0 \\ 0 \\ 0 \\ 0 \\ \left(\frac{\Lambda_E}{\mu_E L_0} - \frac{S_E}{L_0 + \epsilon L_W} \right) \beta_E L_W \end{bmatrix}. \tag{42}$$

Assume that $G_J = G_0/\mu_J$ and $\mu_J \in [0, 1]$. It is clear that $\widehat{G}(X, Z) \geq 0$ for all $(X, Z) \in \mathbb{R}_+^{10}$, since $\Lambda_H/\mu_H P_0 \geq S_H/(P_0 + \epsilon I_E)$, $\Lambda_E/\mu_E L_0 \geq S_E/(L_0 + \epsilon L_W)$, and $(\Lambda_H - \mu_H)/\mu_H P_0 \geq (S_H - 1)/(P_0 + \epsilon I_C)$ provided that $\Lambda_H > \mu_H$. It is also clear that A is an M-matrix, since the off diagonal elements of A are nonnegative. We state a theorem which summarizes the above result.

Theorem 2. *The disease-free equilibrium of model system (1) is globally asymptotically stable if $R_0 \leq 1$ and the assumptions (H1) and (H2) are satisfied.*

5. The Endemic Equilibrium State and Its Stability

At the endemic equilibrium humans are infected by copepods that have been infected by first-stage larvae (L_W). The endemic equilibrium point of the model system (1) given by

$$\widehat{E}_1 = \left(S_H^*, I_H^*, I_C^*, W_M^*, W_F^*, G_J^*, E_W^*, L_W^*, S_E^*, I_E^* \right) \tag{43}$$

satisfies

$$\begin{aligned} 0 &= \Lambda_H - \lambda_H^* S_H^* - \mu_H S_H^* + \alpha_H I_H^*, \\ 0 &= \lambda_H^* S_H^* - (\mu_H + \delta_H + \alpha_H) I_H^*, \end{aligned}$$

$$
\begin{aligned}
0 &= \lambda_h^* S_h^* - \mu_C G_J^* I_C^* - \alpha_C I_C^*,\\
0 &= N_C \mu_C G_J^* I_C^* - (\alpha_M + \mu_M) W_M^*,\\
0 &= \frac{\alpha_M}{2} W_M^* - (\mu_F + \alpha_F) W_F^*,\\
0 &= G_0 + \alpha_J G_J^* I_C^* - \mu_J G_J^*,\\
0 &= \alpha_F W_F^* I_h^* - (\mu_W + \alpha_W) E_W^*,\\
0 &= N_W \alpha_W E_W^* - \mu_L L_W^*,\\
0 &= \Lambda_E - \lambda_E^* S_E^* - \mu_E S_E^*,\\
0 &= \lambda_E^* S_E^* - (\mu_E + \delta_E) I_E^*,
\end{aligned}
\tag{44}
$$

for all $S_H^*, I_H^*, I_C^*, W_M^*, W_F^*, G_J^*, E_W^*, L_W^*, S_E^*, I_E^* > 0$. We therefore obtain the following endemic values. The endemic value of susceptible humans is given by

$$
S_H^* = \frac{\Lambda_H + \alpha_H I_H^*}{(\lambda_H^* + \mu_H)}. \tag{45}
$$

From (45) we note that the susceptible human population at endemic equilibrium is proportional to the average time of stay in the susceptible class and the rate at which new susceptible individuals are entering the susceptible class either through birth or through infected individuals who recover from the disease. Individuals leave the susceptible class through either infection or death. The endemic value of infected humans is given by

$$
I_H^* = \frac{\lambda_H^* S_H^*}{(\mu_H + \delta_H + \alpha_H)}. \tag{46}
$$

We note from (46) that the population of infected humans at the endemic equilibrium point is proportional to the average time of stay in the infected class, the rate at which susceptible individuals become infected, and the density of susceptible individuals. The endemic value of infected copepods population within a single infected human at the equilibrium point is given by

$$
I_C^* = \frac{\lambda_H^* (S_H^* - 1)}{(I_H^* + 1)(\mu_C G_J^* + \alpha_C)}, \tag{47}
$$

where $S_H^* > 1$. From (47) we note that the average infected copepod population within a single infected human is proportional to the average life-span of infected copepods within a single infected human host and the rate of infection of a single susceptible individual to become infected. We also note that this expression provides a link between the dynamics of the infected copepods within-host and human population dynamics. The endemic value of mature worm population within a single infected human is given by

$$
W_M^* = \frac{N_C \mu_C G_J^* I_C^*}{(\alpha_M + \mu_M)}. \tag{48}
$$

We note from (48) that the population of mature worms within a single infected human at endemic equilibrium point is proportional to the average life-span of mature worms and the rate at which mature worms are released after infected copepods within human host have been killed by human gastric juice. The endemic value of fertilized female worm population within a single infected human is given by

$$
W_F^* = \frac{1}{2} \frac{\alpha_M W_M^*}{(\alpha_F + \mu_F)}. \tag{49}
$$

The average population of fertilized female worms within an infected human at endemic equilibrium point is equal to the average life-span of female worms and the rate at which mature worms become fertilized female worms. The endemic value of a single human gastric juice is given by

$$
G_J^* = \frac{G_0}{(\mu_J - \alpha_J I_C^*)}, \tag{50}
$$

where $\mu_J > \alpha_J I_C^*$. The endemic value of Guinea worm eggs population in the physical water environment is given by

$$
E_W^* = \frac{\alpha_F W_F^* (I_H^* + 1)}{(\alpha_W + \mu_W)}. \tag{51}
$$

We note from (51) that the worm egg population at equilibrium point is proportional to the average life-span of eggs, the rate at which each infected human host excretes Guinea worm eggs, and the total number of infected humans. The endemic value of Guinea worm larva population in the physical water environment is given by

$$
L_W^* = \frac{N_W \alpha_W E_W^*}{\mu_L}. \tag{52}
$$

We note from (52) that the larvae population at equilibrium point is proportional to the rate at which Guinea worm eggs hatch, the number of larvae generated by each egg, and the average life-span of larvae. The value of susceptible copepod population at equilibrium point is given by

$$
S_E^* = \frac{\Lambda_E}{(\lambda_E^* + \mu_E)}. \tag{53}
$$

From (53) we note that susceptible copepod population at endemic equilibrium is proportional to the average time of stay in susceptible copepod class and the rate at which new susceptible copepods are entering the susceptible copepod class through birth. The endemic value of infected copepod population is given by

$$
I_E^* = \frac{\lambda_E^* S_E^*}{(\delta_E + \mu_E)} = \frac{\lambda_E^* \Lambda_E}{(\lambda_E^* + \mu_E)(\delta_E + \mu_E)}. \tag{54}
$$

We note from (54) that infected copepod population at the endemic equilibrium point is proportional to the average time of stay in the infected copepod class, the rate at which susceptible copepods become infected, and the density of susceptible copepods. We also make the endemic equilibrium of the model system (1) given by expressions (45)–(54) depend

on both within-host and between-host disease parameters.

5.1. Existence of the Endemic Equilibrium State. In this section we present some results concerning the existence of an endemic equilibrium solution for the model system (1). To determine the existence and uniqueness of the endemic equilibrium point (EEP) of the model system (1), we can easily express S_H^*, I_H^*, I_C^*, W_M^*, W_F^*, E_W^*, and L_W^* in terms of I_E^* in the form

$$
\begin{aligned}
S_H^*\left(I_E^*\right) &= \frac{\left[\Lambda_H\left(a_1 + a_2 I_E^*\right) + \alpha_H a_0 I_E^*\right]\left(P_0 + \epsilon I_E^*\right)}{\left(a_1 + a_2 I_H^*\right)\left[\beta_H I_E^* + \mu_H\left(P_0 + \epsilon I_E^*\right)\right]},\\
I_H^*\left(I_E^*\right) &= \frac{a_0 I_E^*}{a_1 + a_2 I_E^*},\\
I_C^*\left(I_E^*\right) &= \frac{I_E^*\left[\beta_H\left(\Lambda_H - \mu_H\right) Z_E^{(a)} + Z_E^{(b)}\beta_H I_E^*\right]}{\left(P_0 + \epsilon I_E^*\right)\left(\mu_{CH} G_J^* + \alpha_C\right)\left(I_H^* + 1\right) Z_E^{(c)}},\\
W_M^*\left(I_E^*\right) &= \frac{N_C \mu_C G_J^* I_E^*\left[\beta_H\left(\Lambda_H - \mu_H\right) Z_E^{(a)} + Z_E^{(b)}\beta_H I_E^*\right]}{\left(\alpha_M + \mu_M\right)\left(P_0 + \epsilon I_E^*\right)\left(\mu_C G_J^* + \alpha_C\right)\left(I_H^* + 1\right) Z_E^{(c)}},\\
W_F^*\left(I_E^*\right) &= \frac{1}{2}\frac{\alpha_M N_C \mu_C G_J^* I_E^*\left[\beta_H\left(\Lambda_H - \mu_H\right) Z_E^{(a)} + Z_E^{(b)}\beta_H I_E^*\right]}{\left(\alpha_F + \mu_F\right)\left(\alpha_M + \mu_M\right)\left(P_0 + \epsilon I_E^*\right)\left(\mu_{CH} G_J^* + \alpha_C\right)\left(I_H^* + 1\right) Z_E^{(c)}},\\
E_W^*\left(I_E^*\right) &= \frac{\alpha_F \alpha_M N_C \mu_C G_J^* I_E^*\left[\beta_H\left(\Lambda_H - \mu_H\right) Z_E^{(a)} + Z_E^{(b)}\beta_H I_E^*\right]}{2\left(\alpha_W + \mu_W\right)\left(\alpha_F + \mu_F\right)\left(\alpha_M + \mu_M\right)\left(P_0 + \epsilon I_E^*\right)\left(\mu_{CH} G_J^* + \alpha_C\right) Z_E^{(c)}},\\
L_W^*\left(I_E^*\right) &= \frac{Q_E G_J^*}{\left(\mu_C G_J^* + \alpha_C\right)} \cdot \frac{\beta_H\left(\Lambda_H - \mu_H\right) I_E^* Z_E^{(a)} + Z_E^{(b)}\beta_H I_E^{*2}}{\left(P_0 + \epsilon I_E^*\right) Z_E^{(c)}},
\end{aligned}
\tag{55}
$$

where

$$
\begin{aligned}
Z_E^{(a)} &= \left(a_1 + a_2 I_E^*\right)\left(P_0 + \epsilon I_E^*\right),\\
Z_E^{(b)} &= \Lambda_H \alpha_H a_0\left(P_0 + \epsilon I_E^*\right) - \left(a_1 + a_2 I_E^{*2}\right)\beta_H,\\
Z_E^{(c)} &= \left(a_1 + a_2 I_E^*\right)\left(\beta_H I_E^* + \mu_H\left(P_0 + \epsilon I_E^*\right)\right),\\
Q_E &= \frac{1}{2}\cdot\frac{N_C \mu_C}{\mu_L}\cdot\frac{N_W \alpha_W}{\left(\mu_W + \alpha_W\right)}\cdot\frac{\alpha_F}{\left(\mu_F + \alpha_F\right)}\\
&\quad\cdot\frac{\alpha_M}{\left(\mu_M + \alpha_M\right)},
\end{aligned}
$$

$$
\begin{aligned}
a_0 &= \beta_H \Lambda_H,\\
a_1 &= \mu_H P_0\left(\mu_H + \delta_H + \alpha_H\right),\\
a_2 &= \beta_H\left(\mu_H + \delta_H\right)\mu_H \epsilon\left(\mu_H + \delta_H + \alpha_H\right).
\end{aligned}
\tag{56}
$$

Substituting the expression $\lambda_E = \beta_E L_W/(L_0 + \epsilon L_W)$ and $L_W^* = Q_E G_J^*/(\mu_C G_J^* + \alpha_C)\cdot((\beta_H(\Lambda_H - \mu_H) I_E^* Z_E^{(a)} + Z_E^{(b)}\beta_H I_E^{*2})/(P_0 + \epsilon I_E^*) Z_E^{(c)})$ into (25) we get

$$
I_E^* h\left(I_E^*\right) = I_E^*\left[\gamma_3 I_E^{*3} + \gamma_2 I_E^{*2} + \gamma_1 I_E^* + \gamma_0\right] = 0, \tag{57}
$$

where

$$
\begin{aligned}
\gamma_3 &= \frac{G_J^*\left(\mu_C G_0 + \mu_J \alpha_C\right)\left(\beta_E + \epsilon\mu_E\right) L_0 \mu_E P_0 \mu_H \epsilon}{\beta_E \Lambda_E G_0\left(\mu_C G_J^* + \alpha_C\right)} R_0^2\left[a_2\left(\beta_H - \mu_H\right) + a_2\left(\beta_H + \mu_H \epsilon\right)\mu_E L_0 - \beta_H \Lambda_H \alpha_H a_0\right] > 0,\\
\gamma_1 &= \frac{G_J^*\left(\mu_C G_0 + \mu_J \alpha_C\right)\left(\beta_E + \epsilon\mu_E\right) L_0 \mu_E\left(\mu_E + \delta_H\right) P_0^2 \mu_H\left(a_1 + \Lambda_H \alpha_H a_0\right)}{\beta_E \Lambda_E G_0\left(\mu_C G_J^* + \alpha_C\right)} R_0^2
\end{aligned}
$$

$$+ a_1 \left[1 - \frac{\beta_H (\mu_E + \delta_E)(\mu_C G_0 + \mu_J \alpha_C)}{G_0} R_0^2\right] + P_0 \mu_E L_0 a_2 (\beta_H + \mu_H \epsilon)$$

$$- \frac{L_0 \mu_E P_0 \mu_H (\mu_C G_0 + \mu_J \alpha_C) G_J^*}{G_0 (\mu_C G_J^* + \alpha_C)} \left[a_1 \epsilon + a_2 P_0 + \frac{\Lambda_H G_0 \epsilon}{(\Lambda_H - \mu_H)}\right],$$

$$\gamma_2 = B\beta_H (\Lambda_H - \mu_H) \left[a_1 \epsilon + a_2 P_0 + \frac{a_2 \mu_E L_0 (\beta_H + \epsilon \mu_E)}{(\Lambda_H - \mu_H)}\right] + A\beta_H [\beta_H - (\Lambda_H - \mu_H)\epsilon],$$

$$\gamma_0 = \mu_E L_0 \mu_H a_1 P_0 \left[1 - \frac{G_J^* (\mu_C G_0 + \mu_J \delta_C)}{(\mu_C G_J^* + \alpha_C) G_0} R_0^2\right] - \frac{G_J^* (\mu_C G_0 + \mu_J \alpha_C) L_0 \mu_E P_0^2 \mu_H \beta_H}{(\Lambda_H - \mu_H) G_0 (\mu_C G_J^* + \alpha_C)} \left[\mu_H (\mu_H + \delta_H + \alpha_H) - \Lambda_H^2 \alpha_H\right] R_0^2,$$

$$A = \frac{Q_E G_J^* \beta_E \Lambda_E}{(\mu_C G_J^* + \alpha_C)(\mu_E + \delta_E)},$$

$$B = \frac{Q_E G_J^* (\beta_E + \epsilon \mu_E)}{(\mu_C G_J^* + \alpha_C)}. \tag{58}$$

We can easily note that (57) gives $I_E^* = 0$, which corresponds to the disease-free equilibrium and

$$h(I_E^*) = \gamma_3 I_E^{*3} + \gamma_2 I_E^{*2} + \gamma_1 I_E^* + \gamma_0 = 0, \tag{59}$$

which corresponds to the existence of endemic equilibria. Solving for I_E^* in $h(I_E^*) = 0$, the roots of $h(I_E^*) = 0$ are determined by using Descartes's rule of sign. The various possibilities are tabulated in Table 2.

We summarize the results in Table 2 in the following Theorem 3.

Theorem 3. *The model system (1)*

(1) *has a unique endemic equilibrium whenever Cases 1, 2, 3, 4, 5, 6, 7, and 8 are satisfied and if* $R_0 > 1$,

(2) *could have more than one endemic equilibrium if Case 8 is satisfied and* $R_0 > 1$,

(3) *could have two endemic equilibria if Cases 3, 5, and 7 are satisfied.*

We now employ the center manifold theory [22] to establish the local asymptotic stability of the endemic equilibrium of model system (1).

5.2. Local Stability of the Endemic Equilibrium. We determine the local asymptotic stability of the endemic steady state of the model system (1) by using the center manifold theory described in [22]. In our case, we use center manifold theory by making the following change of variables. Let $S_H = x_1$, $I_H = x_2$, $I_C = x_3$, $W_M = x_4$, $W_F = x_5$, $G_J = x_6$, $E_W = x_7$, $E_W = x_8$, $S_E = x_9$, and $I_E = x_{10}$. We also use the vector notation $\mathbf{x} = (x_1, x_2, x_3, x_4, x_5, x_6, x_7, x_8, x_9, x_{10})^T$ so that the model system (1) can be written in the form

$$\frac{d\mathbf{x}}{dt} = \mathbf{f}(\mathbf{x}, \beta^*), \tag{60}$$

where

$$\mathbf{f} = (f_1, f_2, f_3, f_4, f_5, f_6, f_7, f_8, f_9, f_{10}). \tag{61}$$

Therefore, model system (1) can be rewritten as

$$\begin{aligned}
\dot{x}_1 &= \Lambda_H - \lambda_H x_1 - \mu_H x_1 + \alpha_H x_2,\\
\dot{x}_2 &= \lambda_H x_1 - (\mu_H + \delta_H + \alpha_H) x_2,\\
\dot{x}_3 &= \frac{\lambda_H (x_1 - 1)}{x_2 + 1} - (\mu_C x_6 + \alpha_C) x_3,\\
\dot{x}_4 &= N_C \mu_C x_6 x_3 - (\alpha_M + \mu_M) x_4,\\
\dot{x}_5 &= \frac{\alpha_M}{2} x_4 - (\mu_F + \alpha_F) x_5,\\
\dot{x}_6 &= G_0 + \alpha_J x_6 x_3 - \mu_J x_6,\\
\dot{x}_7 &= \alpha_F x_5 (x_2 + 1) - (\mu_W + \alpha_W) x_7,\\
\dot{x}_8 &= N_W \alpha_W x_7 - \mu_L x_8,\\
\dot{x}_9 &= \Lambda_E - \lambda_E x_9 - \mu_E x_9,\\
\dot{x}_{10} &= \lambda_E x_9 - (\mu_E + \delta_E) x_{10},
\end{aligned} \tag{62}$$

where

$$\lambda_H = \frac{\beta^* x_{10}}{P_0 + \epsilon x_{10}},$$
$$\lambda_E = \frac{k\beta^* x_8}{L_0 + \epsilon x_8}. \tag{63}$$

The method involves evaluating the Jacobian matrix of system (62) at the disease-free equilibrium E^0 denoted by $J(E^0)$. The Jacobian matrix associated with the system of (62) evaluated at the disease-free equilibrium (E_0) is given by

$$J(E_0) = \begin{pmatrix} -\mu_H & \alpha_H & 0 & 0 & 0 & 0 & 0 & 0 & 0 & -\frac{\beta_H \Lambda_H}{\mu_H P_0} \\ 0 & b_0 & 0 & 0 & 0 & 0 & 0 & 0 & 0 & \frac{\beta_H \Lambda_H}{P_0 \mu_H} \\ 0 & 0 & b_1 & 0 & 0 & 0 & 0 & 0 & 0 & \frac{\beta_H (\Lambda_H - \mu_H)}{\mu_H P_0} \\ 0 & 0 & \frac{N_C \mu_C G_0}{\mu_J} & b_2 & 0 & 0 & 0 & 0 & 0 & 0 \\ 0 & 0 & 0 & \frac{\alpha_M}{2} & b_3 & 0 & 0 & 0 & 0 & 0 \\ 0 & 0 & \alpha_J \frac{G_0}{\mu_J} & 0 & 0 & -\mu_J & 0 & 0 & 0 & 0 \\ 0 & 0 & 0 & 0 & \alpha_F & 0 & b_4 & 0 & 0 & 0 \\ 0 & 0 & 0 & 0 & 0 & 0 & N_W \alpha_W & -\mu_L & 0 & 0 \\ 0 & 0 & 0 & 0 & 0 & 0 & 0 & -\frac{\beta_E \Lambda_E}{\mu_E L_0} & -\mu_E & 0 \\ 0 & 0 & 0 & 0 & 0 & 0 & 0 & \frac{\beta_E \Lambda_E}{\mu_E L_0} & 0 & b_5 \end{pmatrix}, \tag{64}$$

where

$$b_0 = -(\mu_H + \delta_H + \alpha_H),$$
$$b_1 = -\frac{(\mu_C G_0 + \mu_J \alpha_C)}{\mu_J},$$
$$b_2 = -(\mu_M + \alpha_M),$$
$$b_3 = -(\mu_F + \alpha_F),$$
$$b_4 = -(\mu_W + \alpha_W),$$
$$b_5 = -(\mu_E + \alpha_E). \tag{65}$$

By using the similar approach from Section 4.1, the basic reproductive number of model system (62) is

$$R_0 = \sqrt{\frac{1}{2} \cdot \frac{\alpha_M}{\alpha_M + \mu_M} \cdot \frac{\alpha_F}{\alpha_F + \mu_F} \cdot \frac{N_C \mu_C G_0}{\mu_C G_0 + \mu_J \alpha_C} \cdot \frac{\beta_H (\Lambda_H - \mu_H)}{P_0 \mu_H} \cdot \frac{N_W \alpha_W}{(\alpha_W + \mu_W) \mu_L} \frac{\beta_E \Lambda_E}{\mu_E (\mu_E + \delta_E) L_0}}. \tag{66}$$

Now let us consider $\beta_E = k\beta_H$, regardless of whether $k \in (0, 1)$ or $k \geq 1$, and let $\beta_H = \beta^*$. Taking β^* as the bifurcation parameter and if we consider $R_0 = 1$ and solve for β^* in (66), we obtain

$$\beta^* = \sqrt{\frac{2L_0 (\mu_E + \delta_E) \mu_E (\mu_W + \alpha_W) \mu_L (\mu_M + \alpha_M) (\mu_F + \alpha_F) (\mu_C G_0 + \alpha_C \mu_J) P_0 \mu_H}{k \alpha_F \alpha_M N_C \mu_C G_0 N_W \alpha_W (\Lambda_H - \mu_H) \Lambda_E}}. \tag{67}$$

Note that the linearized system of the transformed equations (62) with bifurcation point β^* has a simple zero eigenvalue. Hence, the center manifold theory [22] can be used to analyse the dynamics of (62) near $\beta_H = \beta^*$.

Table 2: Number of possible positive roots of $h(I_E^*) = 0$.

Cases	γ_3	γ_2	γ_1	γ_0	Number of sign changes	Number of possible real roots (endemic equilibrium)
1	+	+	+	+	0	0
2	+	+	+	−	1	1
3	+	+	−	+	2	0, 2
4	+	+	−	−	1	1
5	+	−	−	+	2	0, 2
6	+	−	−	−	1	1
7	+	−	+	+	2	0, 2
8	+	−	+	−	3	1, 3

In particular, Theorem 4.1 in Castillo-Chavez and Song [23], reproduced below as Theorem 4 for convenience, will be used to show the local asymptotic stability of the endemic equilibrium point of (62) (which is the same as the endemic equilibrium point of the original system (1), for $\beta_H = \beta^*$).

Theorem 4. *Consider the following general system of ordinary differential equations with parameter ϕ:*

$$\frac{dx}{dt} = f(x, \phi), \qquad f : \mathbf{R}^n \times \mathbf{R} \longrightarrow \mathbf{R}, \ f : \mathbf{C}^2\left(\mathbf{R}^2 \times \mathbf{R}\right), \tag{68}$$

where 0 is an equilibrium of the system, that is, $f(0, \phi) = 0$ for all ϕ, and assume that

(A1) *$A = D_x f(0,0) = ((\partial f_i/\partial x_j)(0,0))$ is a linearization matrix of the model system (68) around the equilibrium 0 with ϕ evaluated at 0. Zero is a simple eigenvalue of A, and other eigenvalues of A have negative real parts,*

(A2) *matrix A has a right eigenvector u and a left eigenvector v corresponding to the zero eigenvalue.*

Let f_k be the kth component of f and

$$a = \sum_{k,i,j=1}^{n} u_k v_i v_j \frac{\partial^2 f_k}{\partial x_i \partial x_j}(0,0), \qquad b = \sum_{k,i=1}^{n} u_k v_i \frac{\partial^2 f_k}{\partial x_i \partial \phi}(0,0). \tag{69}$$

The local dynamics of (68) around 0 are totally governed by a and b and are summarized as follows.

(i) *$a > 0$ and $b > 0$. When $\phi < 0$ with $|\phi| \ll 1$, 0 is locally asymptotically stable, and there exists a positive unstable equilibrium; when $0 < \phi \ll 1$, 0 is unstable and there exists a negative and locally asymptotically stable equilibrium.*

(ii) *$a < 0$ and $b < 0$. When $\phi < 0$ with $|\phi| \ll 1$, 0 is unstable; when $0 < \phi \ll 1$, 0 is locally asymptotically stable, and there exists a positive unstable equilibrium.*

(iii) *$a > 0$ and $b < 0$. When $\phi < 0$ with $|\phi| \ll 1$, 0 is unstable, and there exists a locally asymptotically stable negative equilibrium; when $0 < \phi \ll 1$, 0 is stable and a positive unstable equilibrium appears.*

(iv) *$a < 0$ and $b > 0$. When ϕ changes from negative to positive, 0 changes its stability from stable to unstable. Correspondingly a negative unstable equilibrium becomes positive and locally asymptotically stable.*

In order to apply Theorem 4, the following computations are necessary (it should be noted that we are using β^* as the bifurcation parameter, in place of ϕ in Theorem 4).

Eigenvectors of J_{β^*}. For the case when $R_0 = 1$, it can be shown that the Jacobian matrix of (62) at $\beta_H = \beta^*$ (denoted by J_{β^*}) has a right eigenvector associated with the zero eigenvalue given by

$$\mathbf{u} = \left[u_1, u_2, u_3, u_4, u_5, u_6, u_7, u_8, u_9, u_{10}, u_{11}, u_{12}\right]^T, \tag{70}$$

where

$$u_1 = \frac{\beta^* \Lambda_H}{\mu_H^2 P_0}\left[\frac{\alpha_H}{(\mu_H + \delta_H + \alpha_H)} - 1\right],$$

$$u_2 = \frac{\beta^* \Lambda_{\mathrm{H}}}{(\mu_H + \delta_H + \alpha_H) P_0 \mu_H},$$

$$u_3 = \frac{\beta^* (\Lambda_H - \mu_H)}{P_0 \mu_H} \frac{\mu_J}{(\mu_C G_0 + \mu_J \alpha_C)},$$

$$u_4 = \frac{N_C \alpha_C G_0}{(\mu_C G_0 + \mu_J \alpha_C)} \cdot \frac{\beta^* (\Lambda_H - \mu_H)}{P_0 \mu_H (\mu_M + \alpha_M)},$$

$$u_5 = \frac{\alpha_M}{2(\mu_M + \alpha_M)(\mu_F + \alpha_F)} \frac{N_C \mu_C G_0}{(\mu_C G_0 + \mu_J \alpha_C)} \cdot \frac{\beta^* (\Lambda_H - \mu_H)}{P_0 \mu_H},$$

$$u_6 = \frac{\alpha_J G_0}{\mu_J (\mu_C G_0 + \mu_J \alpha_C)} \cdot \frac{\beta^* (\Lambda_H - \mu_H)}{P_0 \mu_H},$$

$$u_7 = \frac{\alpha_M \alpha_F}{2(\mu_M + \alpha_M)(\mu_F + \alpha_F)} \frac{N_C \mu_C G_0}{(\mu_C G_0 + \mu_J \alpha_C)} \cdot \frac{\beta^* (\Lambda_H - \mu_H)}{P_0 \mu_H} \frac{1}{(\mu_W + \alpha_W)},$$

$$u_8 = \frac{\alpha_M \alpha_F}{2(\mu_M + \alpha_M)(\mu_F + \alpha_F)} \frac{N_C \mu_C G_0}{(\mu_C G_0 + \mu_J \alpha_C)} \cdot \frac{\beta^* (\Lambda_H - \mu_H)}{P_0 \mu_H} \frac{N_W \alpha_W}{\mu_L (\mu_W + \alpha_W)},$$

$$u_9 = -\frac{\alpha_M \alpha_F}{2(\mu_M + \alpha_M)(\mu_F + \alpha_F)} \frac{N_C \mu_C G_0}{(\mu_C G_0 + \mu_J \alpha_C)} \cdot \frac{\beta^{*2}(\Lambda_H - \mu_H)}{P_0 \mu_H} \frac{N_W \alpha_W}{\mu_L(\mu_W + \alpha_W)} \cdot \frac{k\Lambda_E}{L_0 \mu_E^2}.$$

$$u_{10} = 1. \tag{71}$$

In addition, the left eigenvector of the Jacobian matrix in (64) associated with the zero eigenvalue at $\beta_H = \beta^*$ is given by

$$\mathbf{v} = [v_1, v_2, v_3, v_4, v_5, v_6, v_7, v_8, v_9, v_{10}, v_{11}, v_{12}]^T, \tag{72}$$

where

$$\begin{aligned}
v_1 &= 0,\\
v_2 &= 0\\
v_3 &= 1,\\
v_4 &= \frac{\beta^{*2}(\Lambda_H - \mu_H)}{\mu_H P_0} \cdot \frac{\alpha_F \alpha_M}{2(\mu_F + \alpha_F)(\mu_M + \alpha_M)} \cdot \frac{N_W \alpha_W}{\mu_L(\mu_W + \alpha_W)} \cdot \frac{k\Lambda_E}{\mu_E(\mu_E + \delta_E) L_0},\\
v_5 &= \frac{\beta^{*2}(\Lambda_H - \mu_H)}{\mu_H P_0} \cdot \frac{\alpha_F}{(\mu_F + \alpha_F)} \cdot \frac{N_W \alpha_W}{\mu_L(\mu_W + \alpha_W)} \cdot \frac{k\Lambda_E}{\mu_E(\mu_E + \delta_E) L_0},\\
v_6 &= 0,\\
v_7 &= \frac{\beta^{*2}(\Lambda_H - \mu_H)}{\mu_H P_0} \cdot \frac{N_W \alpha_W}{\mu_L(\mu_W + \alpha_W)} \cdot \frac{k\Lambda_E}{\mu_E(\mu_E + \delta_E) L_0},\\
v_8 &= \frac{\beta^{*2}(\Lambda_H - \mu_H)}{\mu_H P_0} \cdot \frac{1}{\mu_L} \cdot \frac{k\Lambda_E}{\mu_E(\mu_E + \delta_E) L_0},\\
v_9 &= 0,\\
v_{10} &= \frac{\beta^*(\Lambda_H - \mu_H)}{(\mu_E + \delta_E)\mu_H P_0}.
\end{aligned} \tag{73}$$

Computation of Bifurcation Parameters a and b. We evaluate the nonzero second-order mixed derivatives of $\mathbf{f}$ with respect to the variables and β^* in order to determine the signs of a and b. The sign of a is associated with the following nonvanishing partial derivatives of $\mathbf{f}$:

$$\begin{aligned}
\frac{\partial^2 f_1}{\partial x_{10}^2} &= \frac{2\epsilon\beta^* \Lambda_H}{P_0^2 \mu_H},\\
\frac{\partial^2 f_2}{\partial x_{10}^2} &= -\frac{2\epsilon\beta^* \Lambda_H}{P_0^2 \mu_H},\\
\frac{\partial^2 f_3}{\partial x_{10}^2} &= -\frac{2\epsilon\beta^*(\Lambda_H - \mu_H)}{P_0^2 \mu_H},\\
\frac{\partial^2 f_9}{\partial x_8^2} &= \frac{2\epsilon k\beta^* \Lambda_E}{L_0^2 \mu_E},\\
\frac{\partial^2 f_{10}}{\partial x_8^2} &= -\frac{2\epsilon k\beta^* \Lambda_E}{L_0^2 \mu_E}.
\end{aligned} \tag{74}$$

The sign of b is associated with the following nonvanishing partial derivatives of $\mathbf{f}$:

$$\begin{aligned}
\frac{\partial^2 f_1}{\partial x_{10} \partial \beta^*} &= -\frac{\Lambda_H}{\mu_H P_0},\\
\frac{\partial^2 f_2}{\partial x_{10} \partial \beta^*} &= \frac{\Lambda_H}{\mu_H P_0},\\
\frac{\partial^2 f_3}{\partial x_{10} \partial \beta^*} &= \frac{(\Lambda_H - \mu_H)}{\mu_H P_0},\\
\frac{\partial^2 f_9}{\partial x_8 \partial \beta^*} &= -\frac{k\Lambda_E}{\mu_E L_0},\\
\frac{\partial^2 f_{10}}{\partial x_8 \partial \beta^*} &= \frac{k\Lambda_E}{\mu_E L_0}.
\end{aligned} \tag{75}$$

Substituting expressions (71), (73), and (74) into (69), we get

$$\begin{aligned}
a &= u_1 v_{10}^2 \frac{\partial^2 f_1}{\partial x_{10}^2} + u_2 v_{10}^2 \frac{\partial^2 f_2}{\partial x_{10}^2} + u_3 v_{10}^2 \frac{\partial^2 f_3}{\partial x_{10}^2} + u_9 v_8^2 \frac{\partial^2 f_9}{\partial x_8^2} + u_{10} v_8^2 \frac{\partial^2 f_{10}}{\partial x_8^2}\\
&= u_1 v_{10}^2 \left[\frac{2\epsilon\beta^* \Lambda_H}{P_0^2 \mu_H}\right] + u_2 v_{10}^2 \left[\frac{-2\epsilon\beta^* \Lambda_H}{P_0^2 \mu_H}\right] + u_3 v_{10}^2 \left[\frac{-2\epsilon\beta^*(\Lambda_H - \mu_H)}{P_0^2 \mu_H}\right]\\
&\quad + u_9 v_8^2 \left[\frac{2\epsilon k\beta^* \Lambda_E}{L_0^2 \mu_E}\right] + u_{10} v_8^2 \left[\frac{-2\epsilon k\beta^* \Lambda_E}{L_0^2 \mu_E}\right]\\
&= \frac{2\epsilon\beta^* \Lambda_H}{P_0^2 \mu_H} \cdot v_{10}^2 [u_1 - u_2] - u_3 v_{10}^2 \left[\frac{2\epsilon\beta^*(\Lambda_H - \mu_H)}{P_0^2 \mu_H}\right] + \frac{2\epsilon k\beta^* \Lambda_E}{L_0^2 \mu_E} \cdot v_8^2 [u_9 - u_{10}]\\
&< 0
\end{aligned} \tag{76}$$

since $(u_1 - u_2) < 0$, $(u_9 - u_{10}) < 0$, $u_3 > 0$, and $v_{10} > 0$.

Similarly, substituting expressions (71) and (73) and (75) into (69), we get

$$\begin{aligned} b &= u_1 v_{10} \frac{\partial^2 f_1}{\partial x_{10} \partial \beta^*} + u_2 v_{10} \frac{\partial^2 f_2}{\partial x_{10} \partial \beta^*} + u_3 v_{10} \frac{\partial^2 f_3}{\partial x_8 \partial \beta^*} \\ &\quad + u_9 v_8 \frac{\partial^2 f_9}{\partial x_{10} \partial \beta^*} + u_{10} v_8 \frac{\partial^2 f_{10}}{\partial x_8 \partial \beta^*} \\ &= v_{10} \left[\frac{\Lambda_H}{P_0 \mu_H} \cdot u_2 - \frac{\Lambda_H}{P_0 \mu_H} \cdot u_1 + \frac{(\Lambda_H - \mu_H)}{P_0 \mu_H} \cdot u_3 \right] \\ &\quad + \frac{k \Lambda_E}{L_0 \mu_E} \cdot v_8 \left[u_{10} - u_9 \right] \\ &= \frac{\Lambda_H}{P_0 \mu_H} v_{10} \left[u_2 - u_1 \right] + \frac{(\Lambda_H - \mu_H)}{P_0 \mu_H} v_{10} u_3 \\ &\quad + \frac{k \Lambda_E}{L_0 \mu_E} v_8 \left[u_{10} - u_9 \right] \\ &> 0, \end{aligned} \tag{77}$$

since $(u_2 - u_1) > 0$, $(u_{10} - u_9) > 0$, $u_3 > 0$, and $v_{10} > 0$.

Thus, $a < 0$ and $b > 0$. Using Theorem 4, item (iv), we have established the following result which only holds for $R_0 > 1$ but close to 1.

Theorem 5. *The endemic equilibrium guaranteed by Theorem 3 is locally asymptotically stable for $R_0 > 1$ near 1.*

6. Sensitivity Analysis

In this section we carry out sensitivity analysis to evaluate the relative change in basic reproduction number (R_0) when the within-host and between-host parameters as well as the environmental parameters of the model system (1) change. We used the normalized forward sensitivity index of the basic reproduction number, R_0 of the model system (1) to each of the model parameters. The normalized forward sensitivity index of a variable to a parameter is typically defined as "the ratio of the relative change in the variable to the relative change in the parameter" [24]. In this case, if we let R_0 be a differentiable function of the parameter u, then the normalized forward sensitivity index of R_0 at u is defined as

$$\Upsilon_u^{R_0} = \frac{\partial R_0}{\partial u} \times \frac{u}{R_0}, \tag{78}$$

where the quotient u/R_0 is introduced to normalize the coefficient by removing the effect of units [25]. For example, the sensitivity index of R_0 with respect to the human infection rate β_H is given by

$$\Upsilon_{\beta_H}^{R_0} = \frac{\partial R_0}{\partial \beta_H} \times \frac{\beta_H}{R_0} = 0.5. \tag{79}$$

It can be easily noted that the sensitivity index of R_0 with respect to the parameter β_H does not depend on any of the parameter values. The indices of worm larvae death rate within a host and copepods death rate in the physical environment are, respectively, given by

$$\begin{aligned} \Upsilon_{\mu_F}^{R_0} &= -\frac{1}{2} \frac{\mu_F}{(\mu_F + \alpha_F)} = -0.5, \\ \Upsilon_{\mu_E}^{R_0} &= -\frac{1}{2} \frac{(2\mu_E + \delta_E)}{(\mu_E + \delta_E)} = -0.9991. \end{aligned} \tag{80}$$

Using (78)–(80) similar expressions can be derived for the remaining parameters. The resulting sensitivity indices of R_0 to the different model parameters are shown in Table 3. We see from (78)–(80) that the index of parameter β_H is positive and indexes of both parameters μ_L and μ_E are negative. The sign of the index value indicates whether the parameter increases the reproduction number or reduces the reproduction number. Therefore increasing human infection rate β_H reduces R_0 and also increasing μ_L or μ_E reduces R_0. Based on the results shown in Table 3, we observe that the reproduction number R_0 is sensitive to the changes of both the within-host and between-host parameters as well as the environmental parameters (parameters which can be modified by environmental conditions which impact on survival and reproduction of the parasite and vector populations). More specifically, we deduce the following results for the between-host scale:

(i) The reproductive number is most sensitive to the changes of parameter μ_E and the natural death rate of copepods in the physical water environment. This implies that interventions focused on vector control have highest impact on GWD control. Since $\Upsilon_{\mu_E}^{R_0} = -0.9991$, increasing μ_E by 10% decreases the reproduction number by 9.991%. Therefore increasing the death rate of copepods by using chemical such as ABATE or temephos will eventually reduce the transmission of Guinea worm disease.

(ii) The reproductive number also shows significant sensitivity to β_H and β_E since $\Upsilon_{\beta_H}^{R_0} = \Upsilon_{\beta_E}^{R_0} = 0.5$. This implies that reducing human infection rates β_H and β_E by 10% reduces R_0 by 5% for each of these parameters. Therefore, health education to ensure that greater numbers of individuals and communities adopt behavioural practices such as voluntary reporting of GWD cases, prevention of GWD patients from entering drinking water bodies, regular use of water from safe water sources, and, in the absence of such water sources, filtering or boiling water before drinking aimed at preventing transmission of GWD would have high impact in complementing vector control in elimination of GWD.

(iii) Similarly, $\Upsilon_{\alpha_F}^{R_0} = 0.4639$. This implies that reducing the rate at which eggs are excreted in the physical water environment, α_F, by 10% reduces R_0 by 4.639%. Therefore educating people about GWD (i.e., teaching people not to immerse their infected feet into the drinking water when the fertilized female worm is emerging out from their feet or to always filter

Table 3: Sensitivity indices of model reproduction number R_0 to parameters for model system (1), evaluated at the parameters values presented in Tables 4–6.

Parameter	Description	Sensitivity index with positive sign	Sensitivity index with negative sign
μ_E	Natural decay rate of copepods in the water environment		−0.9991
α_C	Natural decay rate of copepods within human host		−0.4853
μ_C	Release rate of mature worms within human host		−0.4853
Λ_H	Human birth rate	+0.50013	
β_H	Human infection rate	+0.5	
N_W	Fecundity rate of worm larvae in the environment	+0.5	
μ_L	Natural decay rate of Guinea worm larvae		−0.5
L_0	Larvae saturation constant		−0.5
N_C	Fecundity rate of mature worm	+0.5	
Λ_E	Copepods birth rate	+0.5	
β_E	Copepods infection rate	+0.5	
P_0	Copepods saturated constant		−0.5
α_H	Human recovery		−0.4998
μ_F	Natural decay rate of fertilized female worms		−0.4639
α_F	Migration rate of fertilized female worms to surface of host's skin	+0.4639	
μ_W	Natural decay rate of worm eggs in the water environment		−0.4545
α_W	Worm egg hatching rate	+0.4545	
μ_M	Natural decay rate of mature worms within human host		−0.25
α_M	Migration rate of mature worms to subcutaneous tissues	+0.25	
μ_J	Dilution/degradation rate of gastric juice		−0.0147
G_0	Supply rate of gastric juice from the source of the body	+0.0147	
δ_E	Induced decay rate of copepods in the water environment		−0.000894

Table 4: Human host parameter values used in simulations.

Parameter	Description	Initial values	Units	Source
Λ_H	Human birth rate	0.1013	People day^{-1}	[14]
β_H	Human infection rate	0.1055	Copepod day^{-1}	Estimated
μ_H	Human natural death rate	2.548×10^{-5}	Day^{-1}	[15, 16]
α_H	Human recovery rate	0.03	Day^{-1}	Estimated
δ_H	GWD induced death rate	4×10^{-8}	Day^{-1}	Estimated

Table 5: Within-host parameter values of the model system (1).

Parameter	Description	Initial values	Units	Source
N_C	Fecundity rate of mature worms	700	People	Estimated
μ_C	Decay rate of copepods within a human host due to gastric juice	0.99	Copepod day^{-1}	Estimated
α_C	Natural death rate of copepods within a human host	0.001	Day^{-1}	Estimated
μ_M	Natural decay rate of mature worms within a human host	0.9	Day^{-1}	Estimated
α_M	Migration rate of mature worms to subcutaneous tissues	0.9	Day^{-1}	Estimated
μ_F	Natural death rate of fertilized female worms within a human host	0.9	Day^{-1}	Estimated
α_F	Migration rate of fertilized female worms to surface of skin	0.07	Day^{-1}	Estimated
μ_J	Dilution/degradation rate of gastric juice	0.05	Day^{-1}	Estimated
α_J	Proliferation rate of gastric juice due to infection	0.4	Day^{-1}	Estimated
G_0	Supply rate of gastric juice from within a human body	1.5	Day^{-1}	Estimated

Table 6: Free-living pathogens and their associated environmental parameter values used in simulations.

Parameter	Description	Initial value	Units	Source
Λ_E	Copepods birth rate	0.75	Copepod day^{-1}	Estimated
β_E	Copepods infection rate	0.7	Larvae day^{-1}	Estimated
μ_E	Natural decay rate of copepods	0.005	Day^{-1}	[15, 16]
δ_E	Disease induced death rate of copepods	9×10^{-6}	Day^{-1}	Estimated
P_0	Copepods saturation constant	20 0000	Day^{-1}	[15, 16]
μ_W	Natural decay rate of Guinea worm eggs	0.333	Day^{-1}	[15, 16]
α_W	Hatching rate of worm eggs	0.009	Day^{-1}	Estimated
N_W	Number of Guinea worm larvae hatched	300	Larvae egg $^{-1}$ day^{-1}	Estimated
μ_L	Natural decay rate of Guinea worm larvae	0.0333	Day^{-1}	[15, 16]
L_0	Larvae saturation constant	5000000	Day^{-1}	[15, 16]
ϵ	Limitation growth rate	0.0991	Day^{-1}	Estimated

contaminated water before drinking the water) will reduce the transmission of the disease.

Further, we also deduce the following results for the within-host scale:

(i) The development of a drug that would kill mature worms within human host would have significant benefits at within-host. However, the drug would have even higher impact if it would kill fertilized female worms.

(ii) The development of interventions that would increase the supply rate of gastric juice would have no benefits in the control of GWD.

Therefore, the lack of drugs to treat GWD has delayed progress in eliminating GWD.

7. Numerical Analysis

The behaviour of model system (1) was investigated using numerical simulations using a Python program version V 2.6 on the Linux operation system (Ubuntu 14.04). The program uses a package odeint function in the scipy.integrate for solving a system of differential equations. The behaviour of the system model (1) was simulated in order to illustrate the analytical results we obtained in this paper. We used parameter values presented in Tables 4–6. Some of the parameter values used in the numerical simulations are from published literature while others were estimated as values of some parameters are generally not reported in literature. The initial conditions used for simulations are given by $S_H(0) = 2500$, $I_H(0) = 10$, $I_C(0) = 0$, $G_J(0) = 1.50$, $W_M(0) = 0$, $W_F(0) = 0$, $S_E(0) = 100000$, $I_E(0) = 0$, $E_W(0) = 0$, and $L_W(0) = 50000$.

Figure 2 illustrates the solution profile of the population of (a) infected humans, (b) infected copepods in the physical water environment, (c) worm eggs in the physical water environment, and (d) worm larvae in the physical water environment, for different values of the infection rate of humans β_H: $\beta_H = 0.1055$, $\beta_H = 0.55$, and $\beta_H = 0.9$. The numerical results show that higher rates of infection at the human population level result in increased population of parasites (worm eggs and worm larvae) in the physical water environment and a noticeable increase in infected copepod population in the physical water environment. Therefore, human behavioural changes which reduce contact with contaminated water bodies through drinking contaminated water reduce transmission of the disease at both human and copepod population level.

Figure 3 illustrates the solution profile of the population of (a) infected humans, (b) infected copepods in the physical water environment, (c) worm eggs in the physical water environment, and (d) worm larvae in the physical water environment, for different values of natural death rate of copepod population in the physical water environment μ_E: $\mu_E = 0.005$, $\mu_E = 0.05$, and $\mu_E = 0.5$. The results show that environmental conditions which increase death of copepods affect transmission of the disease in the human population. Increased death of copepod population reduces transmission risk of the disease at humans population; therefore any mechanisms which enhance the killing of copepod population in the physical water environment reduces transmission risk of GWD within disease endemic communities.

Figure 4 shows graphs of numerical solutions of model system (1) showing propagation of (a) population of infected humans (I_H), (b) population of infected copepods (I_E), (c) population of Guinea worm eggs in the physical water environment, and (d) population of Guinea worm larvae in the physical water environment, for different values of natural death rate of Guinea worm eggs in the physical water environment μ_W: $\mu_W = 0.005$, $\mu_W = 0.5$, and $\mu_W = 0.9$. The results show that the environmental conditions which enhance death of worm eggs affect transmission of GWD in the human population. Increased death of worm egg population reduces transmission risk of the disease at human population level. Therefore any mechanisms which enhance the killing of worm egg population in the physical water environment reduce transmission risk of the disease within GWD endemic communities.

Figure 5 shows graphs of numerical solutions of model system (1) showing propagation of (a) population of infected humans (I_H), (b) population of infected copepods (I_E), (c) population of Guinea worm eggs, and (d) population of Guinea worm larvae in the physical water environment, for different values of natural death rate of Guinea worm larvae in

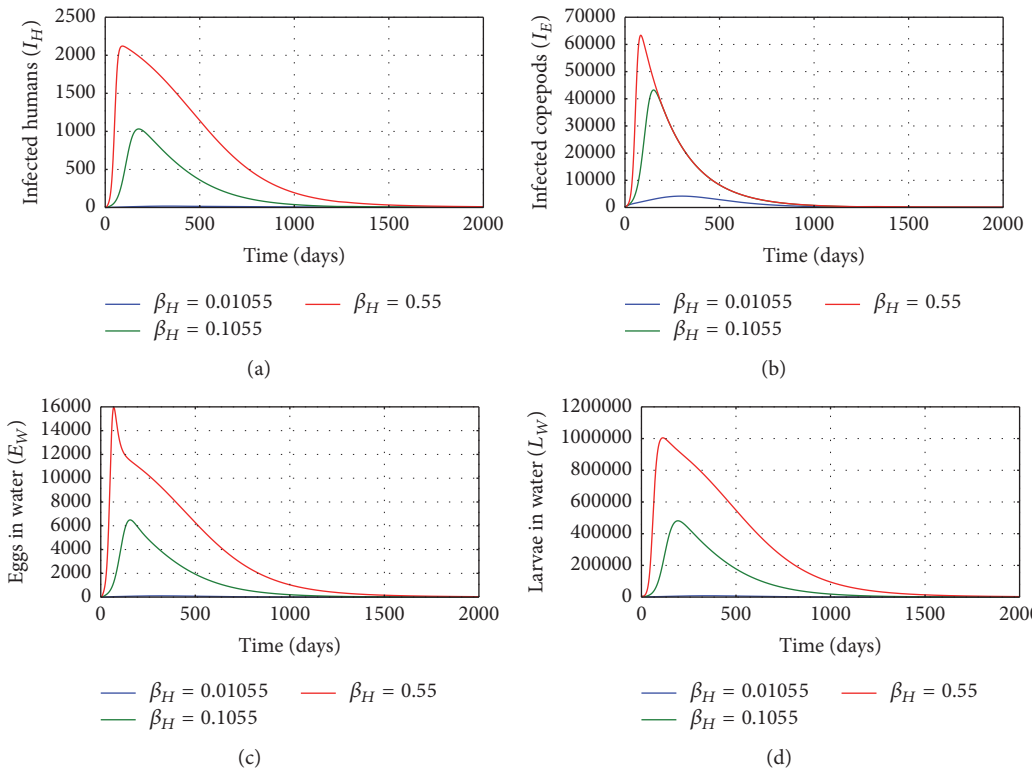

FIGURE 2: Graphs of numerical solutions of model system (1) showing the evolution with time of (a) population of infected humans (I_H), (b) population of infected copepods (I_E), (c) population of Guinea worm eggs in the physical water environment, and (d) population of Guinea worm larvae in the physical water environment, for different values of the infection rate of humans β_H: $\beta_H = 0.1055$, $\beta_H = 0.55$, and $\beta_H = 0.9$.

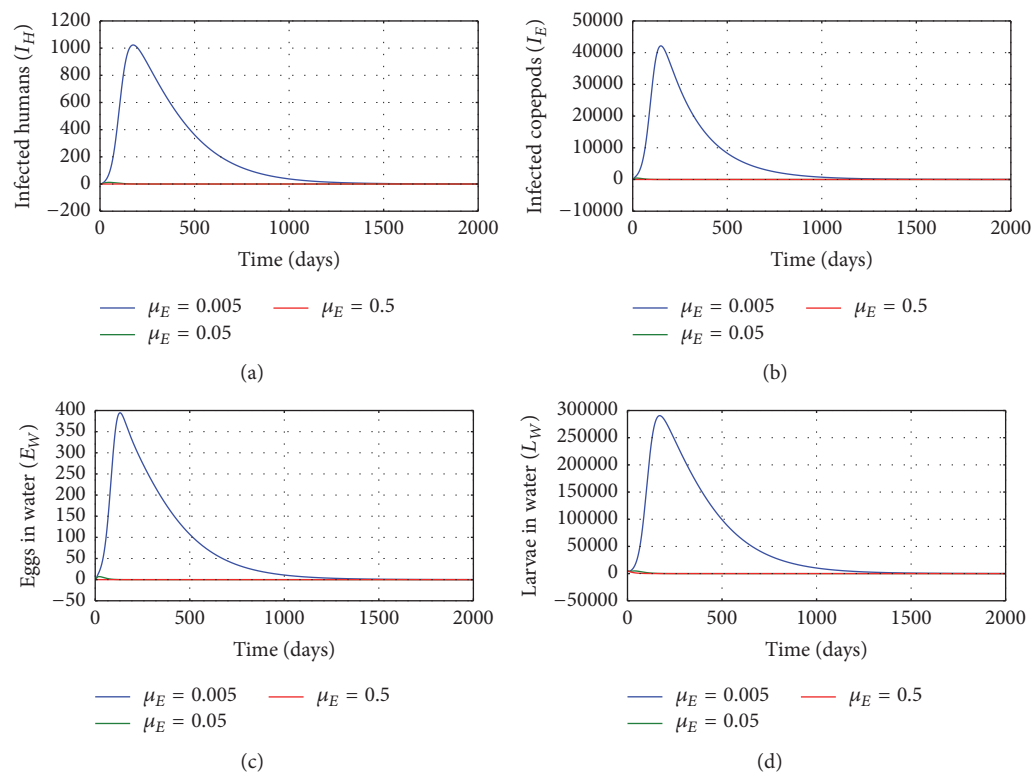

FIGURE 3: Graphs of numerical solutions of model system (1) showing the evolution with time of (a) population of infected humans (I_H), (b) population of infected copepods (I_E), (c) population of Guinea worm eggs in the physical water environment, and (d) population of Guinea worm larvae in the physical water environment, for different values of natural death rate of copepods μ_E: $\mu_E = 0.005$, $\mu_E = 0.05$, and $\mu_E = 0.5$.

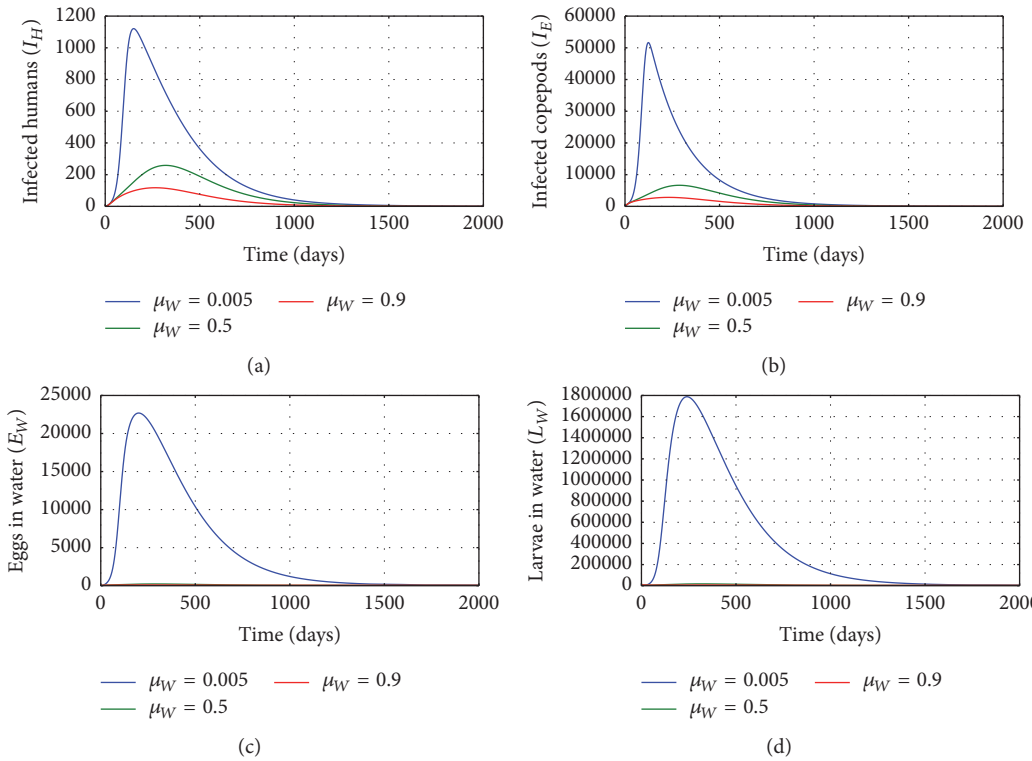

FIGURE 4: Graphs of numerical solutions of model system (1) showing the evolution with time of (a) population of infected humans (I_H), (b) population of infected copepods (I_E), (c) population of Guinea worm eggs in the physical water environment, and (d) population of Guinea worm larvae in the physical water environment, for different values of natural death rate of Guinea worm eggs in the physical water environment μ_W: $\mu_W = 0.005$, $\mu_W = 0.5$, and $\mu_W = 0.9$.

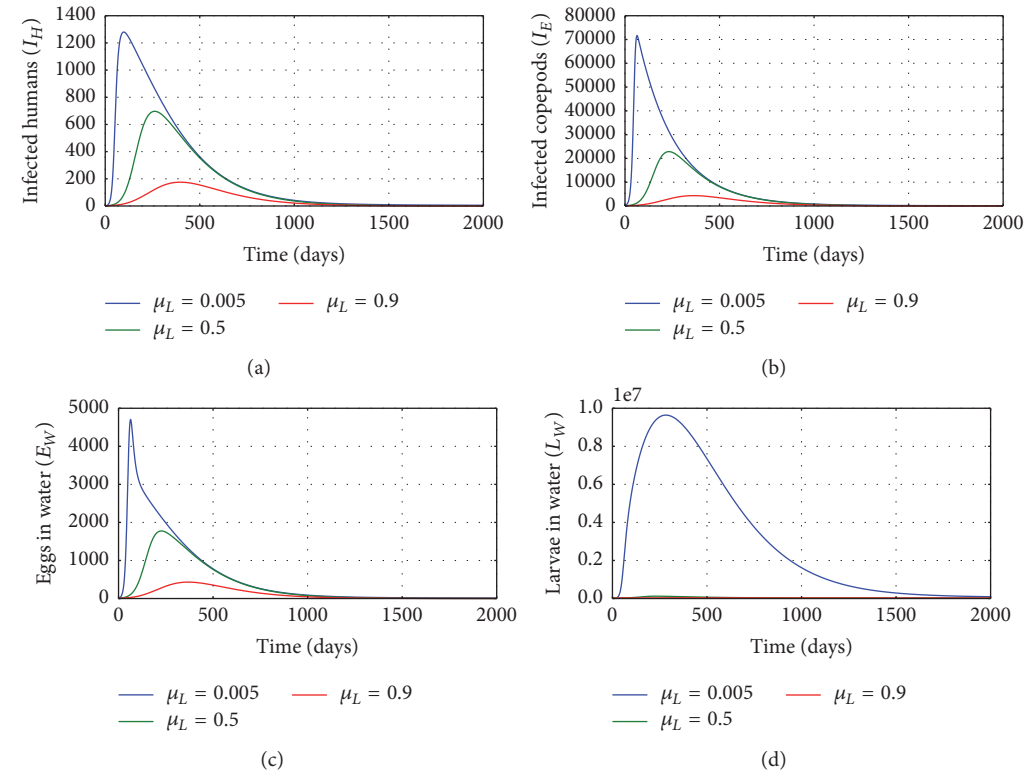

FIGURE 5: Graphs of numerical solutions of model system (1) showing the evolution with time of (a) population of infected humans (I_H), (b) population of infected copepods (I_E), (c) population of Guinea worm eggs, and (d) population of Guinea worm larvae in the physical water environment, for different values of natural death rate of Guinea worm larvae in the physical water environment μ_L: $\mu_L = 0.005$, $\mu_L = 0.5$, and $\mu_L = 0.9$.

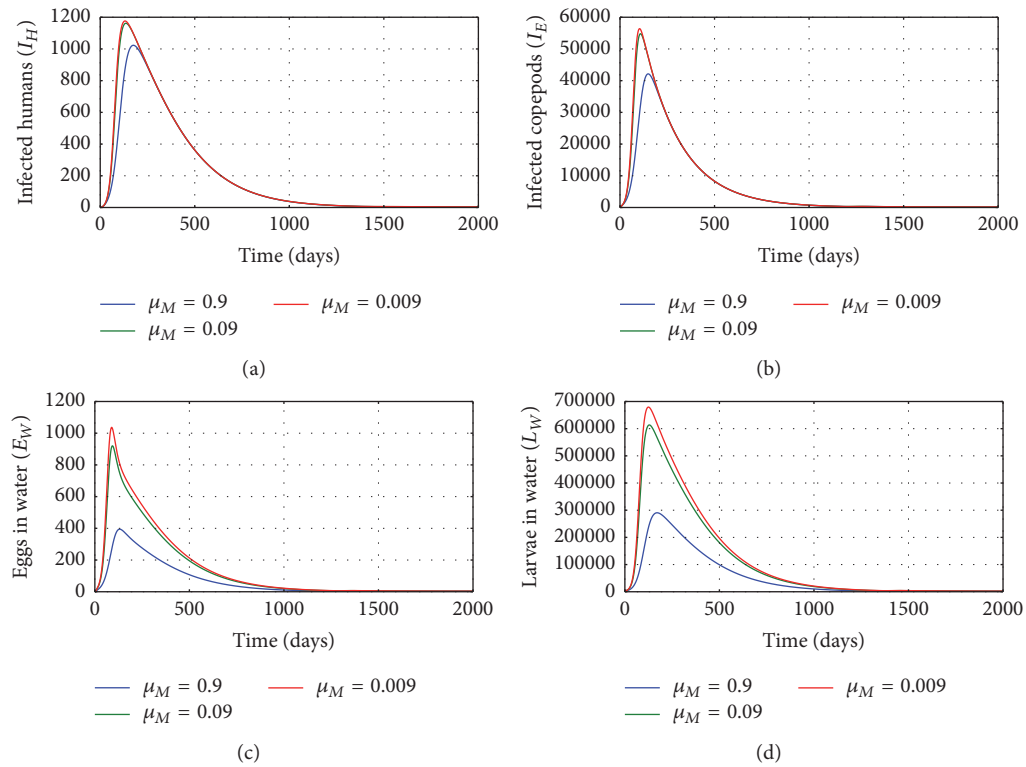

FIGURE 6: Graphs of numerical solutions of model system (1) showing the evolution with time of (a) population of infected humans (I_H), (b) population of infected copepods (I_E), (c) population of Guinea worm eggs in the physical water environment, and (d) population of Guinea worm larvae in the physical water environment, for different values of natural death rate of mature worms inside a single infected human host μ_M: $\mu_M = 0.9$, $\mu_M = 0.09$, and $\mu_M = 0.009$.

the physical water environment μ_L: $\mu_L = 0.005$, $\mu_L = 0.5$, and $\mu_L = 0.9$. The results show that the environmental conditions which increase death of worm larvae reduce transmission of GWD in the human population. Increased death of worm larvae population reduces transmission risk of the disease at human population level. Therefore any interventions which enhance the killing of worm larvae population in the physical water environment reduce transmission risk of GWD within the human population.

Figure 6 shows graphs of numerical solution of model system (1) showing propagation of (a) population of infected humans (I_H), (b) population of infected copepods (I_E), (c) population of Guinea worm eggs in the physical water environment, and (d) population of Guinea worm larvae in the physical water environment, for different values of natural death rate of mature worms inside a single infected human host μ_M: $\mu_M = 0.9$, $\mu_M = 0.09$, and $\mu_M = 0.009$. The results show that the within-host process of death of mature worms affects transmission of the disease in the human population level. Increased death of mature worm population within an infected human host reduces transmission risk of the disease at human population level. Therefore any interventions which enhance the killing of mature worm population inside an infected human host reduce transmission risk of the disease within communities.

Figure 7 shows graphs of numerical solution of model system (1) showing propagation of (a) population of infected humans (I_H), (b) population of infected copepods (I_E), (c) population of Guinea worm eggs, and (d) population of Guinea worm larvae in the physical water environment, for different values of natural death rate of fertilized female worms inside a single infected human host μ_F: $\mu_F = 0.9$, $\mu_F = 0.09$, and $\mu_F = 0.009$. The results show that the within-host processes which increase the death of fertilized female worms can be a potent control measure for GWD. Increased death of fertilized female worms within infected human hosts reduces transmission risk of the disease at human population level. Therefore any interventions which enhance the killing of fertilized female worm population inside an infected human host reduce transmission risk of GWD within a community.

Figure 8 illustrates the solution profiles of the population of (a) infected humans (I_H), (b) infected copepods (I_E) in the physical water environment, (c) worm eggs in the physical water environment, and (d) worm larvae in the physical water environment, for different values of the rate of worm larvae fecundity N_W: $N_W = 30$, $N_W = 300$, and $N_W = 30000$. The results show that an increase of worm larvae produced per day by worm eggs increases the transmission of the disease. Therefore, any interventions which reduce worm larvae fecundity in the physical water environment reduce the transmission risk of the disease in the community.

Figure 9 shows graphs of numerical solution of model system (1) showing the propagation of the population of (a) infected humans (I_H), (b) population of infected copepods (I_E), (c) worm eggs in the physical water environment, and

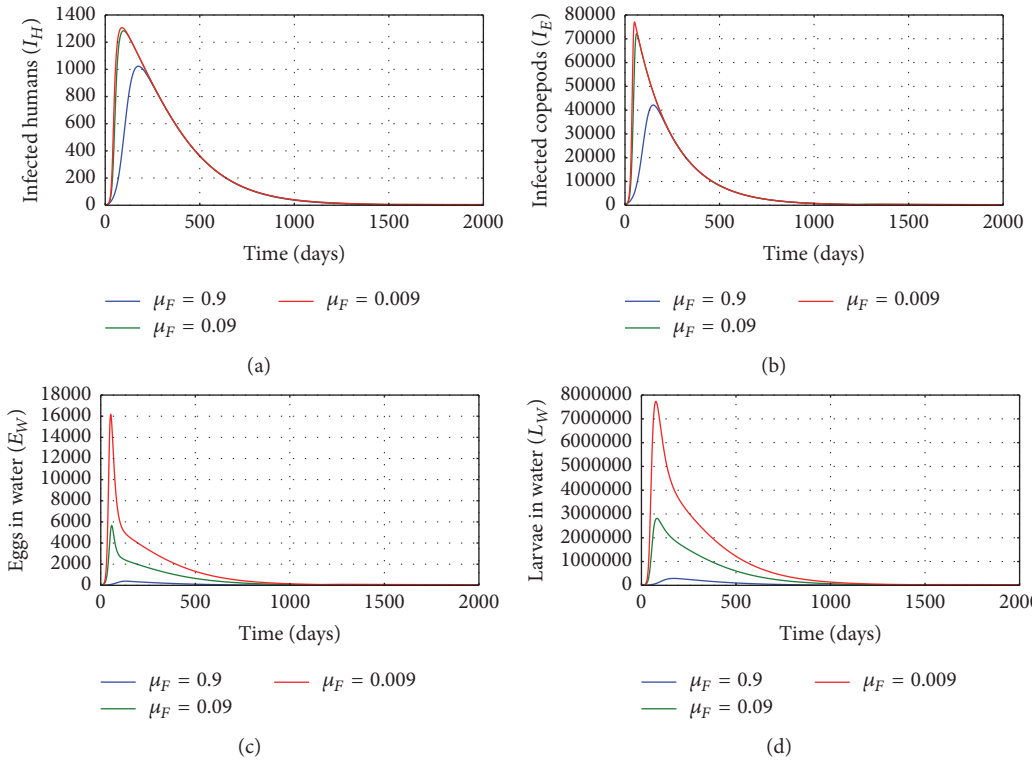

FIGURE 7: Graphs of numerical solutions of model system (1) showing the evolution with time of (a) population of infected humans (I_H), (b) population of infected copepods (I_E), (c) population of Guinea worm eggs, and (d) population of Guinea worm larvae in the physical water environment, for different values of natural death rate of fertilized female worm within a single infected human host μ_F: $\mu_F = 0.9$, $\mu_F = 0.09$, and $\mu_F = 0.009$.

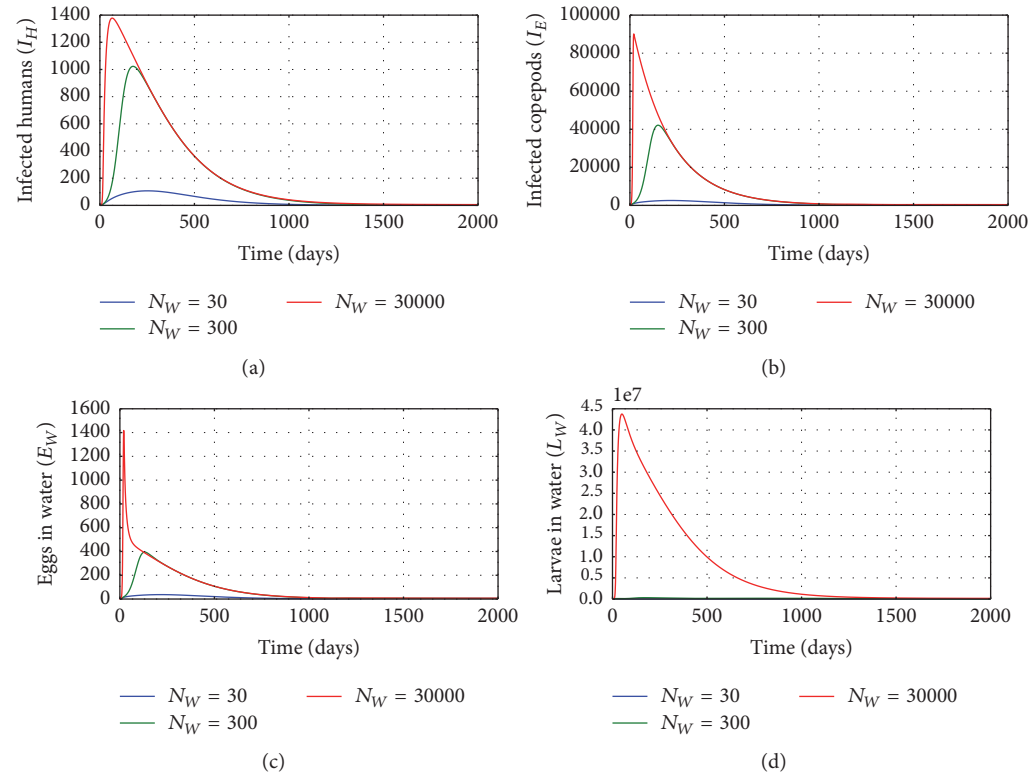

FIGURE 8: Graphs of numerical solutions of model system (1) showing the evolution with time of (a) population of infected humans (I_H), (b) population of infected copepods (I_E), (c) population of Guinea worm eggs in the physical water environment, and (d) population of Guinea worm larvae in the physical water environment, for different values of Guinea worm larvae fecundity N_W: $N_W = 30$, $N_W = 300$, and $N_W = 30000$.

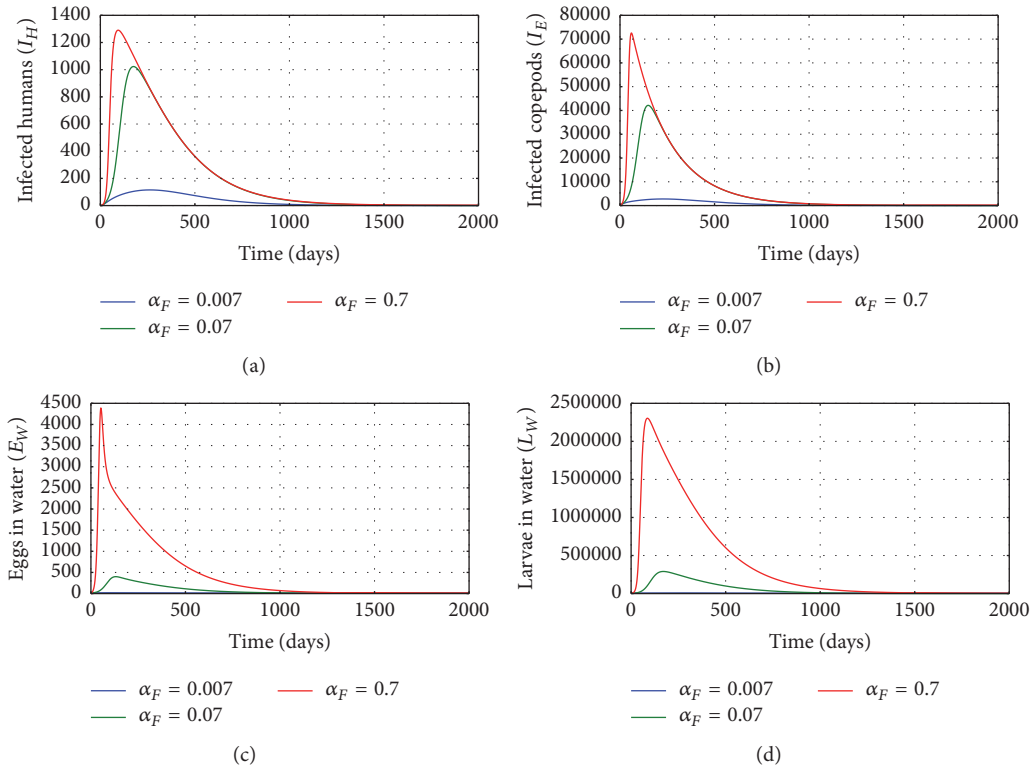

FIGURE 9: Graphs of numerical solutions of model system (1) showing the evolution with time of (a) population of infected humans (I_H), (b) population of infected copepods (I_E), (c) population of Guinea worm eggs in the physical water environment, and (d) population of Guinea worm larvae in the physical water environment, for different values of the rate at which an emerging fertilized female worm from a single infected human host excretes eggs into the physical water environment α_F: $\alpha_F = 0.007$, $\alpha_F = 0.07$, and $\alpha_F = 0.7$.

(d) worm larvae in the physical water environment, for different values of the rate at which an emerging fertilized female worm from a single infected human host excretes number of eggs into the physical water environment α_F: $\alpha_F = 0.007$, $\alpha_F = 0.07$, and $\alpha_F = 0.7$. The results show that higher rate of excretion of worm eggs by each infected human host results in increased population of parasites (worm eggs and worm larvae) in the physical water environment and a noticeable increase in infected copepods. Therefore, improvements in individual sanitation (which reduce contamination of water source with human eggs) are good for the community because they reduce the risk of the disease transmission in the community.

Figure 10 demonstrates numerical solutions showing the propagation of the population of (a) mature worm within infected human host and (b) population of fertilized female worm within infected human host, for different values of the infection rate of humans β_H: $\beta_H = 0.1055$, $\beta_H = 0.01055$, $\beta_H = 0.001055$, and $\beta_H = 0.55$. The results show the influence of between-host disease process on within-host disease process of Guinea worm disease. Here, as transmission rate of GWD in the community increases, the within-host infection intensity of the disease also increases. The numerical results demonstrate that the transmission of the disease at the population level influences the dynamics within an infected individual. Therefore, human behavioural changes (such as filtering water before drinking) which reduce contact with infected copepods reduce infection intensity at individual level. Equally, good sanitation by community which reduces contamination of water bodies reduces the intensity of infection of humans at individual level.

Figure 11 illustrates the graphs of numerical solutions showing the propagation of the population of (a) mature worm within infected human host and (b) population of fertilized female worm within infected human host, for different values of the natural death rate of copepods in the physical water environment μ_E: $\mu_E = 0.005$, $\mu_E = 0.05$, and $\mu_E = 0.5$. The results demonstrate the potency of public health interventions intended to reduce copepods population (such as killing copepods using temephos or boiling the water) on the infection intensity within an infected individual.

Figure 12 illustrates the graphs of numerical solutions showing the propagation of the population of (a) mature worm within infected human host and (b) population of fertilized female worm within infected human host, for different values of the natural death rate of worm larvae in the physical water environment μ_L: $\mu_L = 0.005$, $\mu_L = 0.05$, and $\mu_L = 0.5$. The results demonstrate the influence of public health interventions intended to reduce worm larvae population in the physical water environment (such as destroying worm larvae using chemicals or boiling the water) on the infection intensity within an infected individual. Overall, the numerical results verify the following aspects about GWD transmission dynamics.

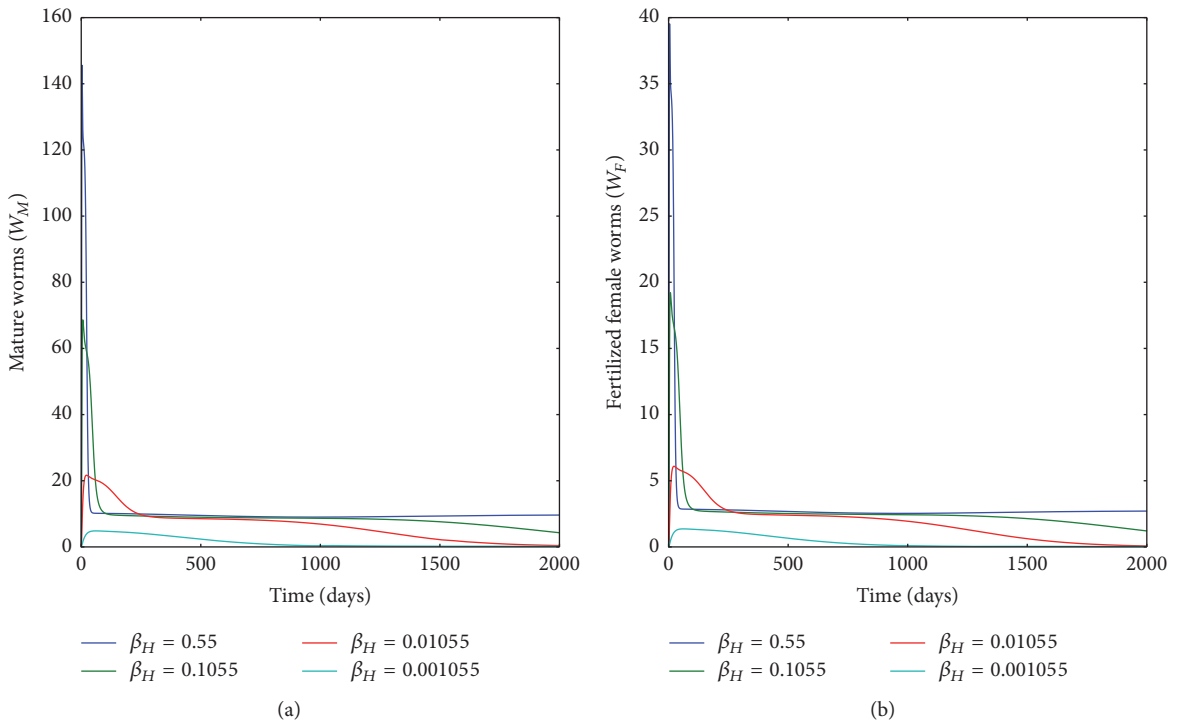

FIGURE 10: Graphs of numerical solutions of model system (1) showing the evolution with time of (a) population of mature worm within infected human host and (b) population of fertilized female worm within infected human host, for different values of the infection rate of humans β_H: $\beta_H = 0.1055$, $\beta_H = 0.01055$, $\beta_H = 0.001055$, and $\beta_H = 0.55$.

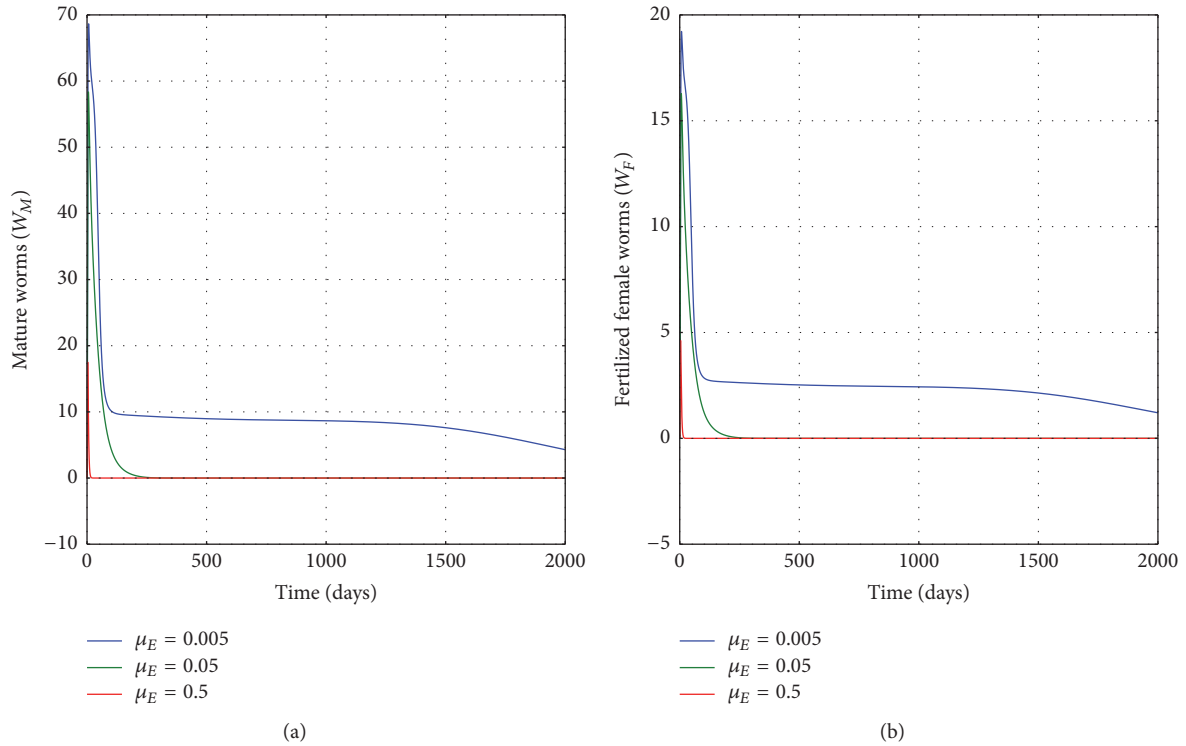

FIGURE 11: Graphs of numerical solutions of model system (1) showing the evolution with time of (a) population of mature worm within infected human host and (b) population of fertilized female worm within infected human host, for different values of the natural death rate of copepods μ_E: $\mu_E = 0.005$, $\mu_E = 0.05$, and $\mu_E = 0.5$.

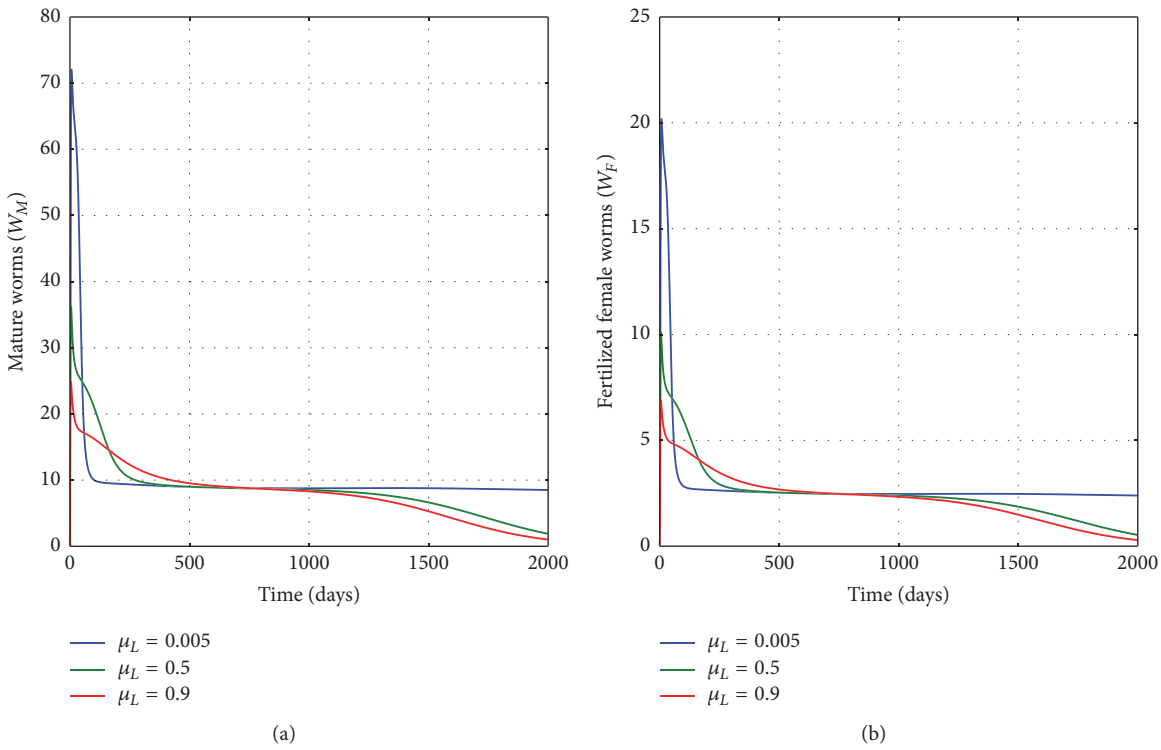

Figure 12: Graphs of numerical solutions of model system (1) showing the evolution with time of (a) population of mature worm within infected human host and (b) population of fertilized female worm within infected human host, for different values of natural death rate of worm larvae in the physical water environment μ_L: $\mu_L = 0.005$, $\mu_L = 0.05$, and $\mu_L = 0.5$.

(i) Higher rates of infection at the human population level result in increased population of parasites (worm eggs and worm larvae) in the physical water environment and a noticeable increase in infected copepod population in the physical water environment.

(ii) Interventions which increase death of copepods through enhanced killing of copepod population in the physical water environment reduce transmission risk of GWD within a disease endemic communities.

(iii) Interventions which enhance death of worm eggs through enhanced killing of worm egg population in the physical water environment reduce transmission risk of the disease within GWD endemic communities.

(iv) Health interventions which increase death of worm larvae in the physical water environment reduce transmission risk of GWD within the human population.

(v) Within-host scale interventions which increase death of mature worm population inside an infected human host reduce transmission risk of the disease within communities.

(vi) Within-host scale interventions which increase the death of fertilized female worms can also be a potent control measure for GWD through reduced transmission risk of GWD within a community.

(vii) An increase in worm fecundity with an infected human host has considerable impact on the transmission of GWD.

(viii) Higher rate of contamination of the physical water environment through excretion of worm eggs by each infected human host results in increased population of parasites (worm eggs and worm larvae) in the physical water environment and a noticeable increase in infected copepods.

(ix) Transmission of the GWD shows reciprocal influence of within-host scale interventions (medical interventions) and between-host scale interventions (public health interventions). Therefore, human behavioural changes (such as filtering water before drinking) which reduce contact with infected copepods reduce infection intensity at individual level. Equally, good sanitation by community which reduces contamination of water bodies reduces the intensity of infection of humans at individual level.

8. Conclusions

Guinea worm disease, like most neglected parasitic diseases, urgently needs renewed attention and sustainable interventions in Africa. The limited scientific knowledge about GWD represents a challenge to the successful elimination of the disease. In this paper, we have sought to identify a broad range of within-host and between-host processes that should

be better understood if GWD is to be eliminated. A multiscale model of GWD transmission dynamics is presented. The multiscale model is shown to be mathematically and epidemiologically well-posed. Sensitivity analyses of the basic reproduction number to the variation of model parameters were carried out. The sensitivity results of the reproduction number show that between-host model parameters (such as infection rate of human host β_H and supply rate of humans Λ_H); within-host model parameters (such as excretion rate of eggs α_F into the physical water environment by each infected human host, fecundity rate of mature worm N_C, decay rate of mature worms μ_M, migration rate of mature worms to the subcutaneous tissue α_M, and decay rate of fertilized worms μ_F); and environmental model parameters (such as the production rate of larvae per egg worm per day α_W, fecundity of larvae N_W generated by eggs, death rate of egg worms μ_W, larva worms μ_L in the physical water environment, supply rate of copepods Λ_E, and decay rate of copepods μ_E) all are responsible for the transmission dynamics of Guinea worm disease within the community. Therefore reducing the infection rate of human, excretion rate of eggs into physical water, and the population of parasites (worm eggs and worm larvae) as well as population of vector host (copepods) in the physical water environment could eventually contribute in eradicating GWD completely from the community.

Conflicts of Interest

The authors declare that they have no conflicts of interest.

Acknowledgments

The authors acknowledge financial support from South Africa National Research Foundation (NRF) Grant no. IPRR (UID 81235) and partial financial support from the Southern African Systems Analysis Centre.

References

[1] S. K. Diamenu and A. A. Nyaku, "Guinea worm disease - A chance for successful eradication in the Volta region, Ghana," *Social Science and Medicine*, vol. 47, no. 3, pp. 405–410, 1998.

[2] S. Watts, "Perceptions and priorities in disease eradication: dracunculiasis eradication in Africa," *Social Science and Medicine*, vol. 46, no. 7, pp. 799–810, 1998.

[3] R. Muller, "Guinea worm disease - The final chapter?" *Trends in Parasitology*, vol. 21, no. 11, pp. 521–524, 2005.

[4] J. M. Hunter, "An introduction to guinea worm on the eve of its departure: dracunculiasis transmission, health effects, ecology and control," *Social Science and Medicine*, vol. 43, no. 9, pp. 1399–1425, 1996.

[5] B. J. Visser, "Dracunculiasis eradication - Finishing the job before surprises arise," *Asian Pacific Journal of Tropical Medicine*, vol. 5, no. 7, pp. 505–510, 2012.

[6] G. Biswas, D. P. Sankara, J. Agua-Agum, and A. Maiga, "Dracunculiasis (guinea worm disease): eradication without a drug or a vaccine.," *Philosophical transactions of the Royal Society of London. Series B, Biological sciences*, vol. 368, no. 1623, p. 20120146, 2013.

[7] S. Cairncross, A. Tayeh, and A. S. Korkor, "Why is dracunculiasis eradication taking so long?" *Trends in Parasitology*, vol. 28, no. 6, pp. 225–230, 2012.

[8] N. C. Iriemenam, W. A. Oyibo, and A. F. Fagbenro-Beyioku, "Dracunculiasis - The saddle is virtually ended," *Parasitology Research*, vol. 102, no. 3, pp. 343–347, 2008.

[9] H. W. Hethcote, "The mathematics of infectious diseases," *SIAM Review*, vol. 42, no. 4, pp. 599–653, 2000.

[10] W. Garira, "The dynamical behaviours of diseases in Africa," in *In Handbook of Systems and Complexity in Health*, pp. 595–623, Springer, New York, 2013.

[11] M. A. Nowak and R. M. May, *Virus Dynamics: Mathematics Principles of Immunology and Virology*, Oxford University Press, London, UK, 2000.

[12] G. Magombedze, W. Garira, and E. Mwenje, "Modelling the human immune response mechanisms to Mycobacterium tuberculosis infection in the lungs," *Mathematical Biosciences and eNgineering*, vol. 3, no. 4, pp. 661–682, 2006.

[13] W. Garira, D. Mathebula, and R. Netshikweta, "A mathematical modelling framework for linked within-host and between-host dynamics for infections with free-living pathogens in the environment," *Mathematical Biosciences*, vol. 256, pp. 58–78, 2014.

[14] J. S. Robert, C. Patrick, H. James, and D. Alex, "A Mathematical Model for the eradication of Guinea worm disease," *Understanding the dynamics of emerging and re-emerging infectious diseases using mathematical models pgs*, pp. 133–156, 2012.

[15] M. O. Adewole, "A Mathematical Model of Dracunculiasis Epidemic and Eradication," *IOSR Journal of Mathematics*, vol. 8, no. 6, pp. 48–56, 2013.

[16] L. Kathryn, "Guinea worm disease (Dracunculiasis): Opening a mathematical can of worms," Tech. Rep., Bryn Mawr College, Pennsylvania, 2012.

[17] B. Hellriegel, "Immunoepidemiology - Bridging the gap between immunology and epidemiology," *Trends in Parasitology*, vol. 17, no. 2, pp. 102–106, 2001.

[18] D. M. Vickers and N. D. Osgood, "A unified framework of immunological and epidemiological dynamics for the spread of viral infections in a simple network-based population," *Theoretical Biology and Medical Modelling*, vol. 4, article no. 49, 2007.

[19] C. Greenaway, "Dracunculiasis (guinea worm disease)," *CMAJ*, vol. 170, no. 4, pp. 495–500, 2004.

[20] C. Castillo-Chavez, Z. Feng, and W. Huang, "On the computation of R0 and its role in global stability. In Mathematical Approaches for Emerging and Re-emerging Infectious Diseases Part 1: An Introduction to Models, Methods and Theory," in *The IMA Volumes in Mathematics and Its Applications*, C. Castillo-Chavez, S. Blower, P. van den Driessche, and., and D. Kirschner, Eds., vol. 125, pp. 229–250, Springer-Verlag, Berlin, 125, 2002.

[21] P. J. Van den Driessche and P. J. Watmough, "Reproduction numbers and sub-threshold endemic equilibria for compartmental models of disease transmission," *Mathematical biosciences*, vol. 180, no. 1, pp. 29–48, 2002.

[22] J. Carr, *Applications of Centre Manifold Theory*, Springer, New York, NY, USA, 1981.

[23] C. Castillo-Chavez and B. Song, "Dynamical models of tuberculosis and their applications," *Mathematical Biosciences and Engineering (MBE)*, vol. 1, no. 2, pp. 361–404, 2004.

[24] N. Chitnis, J. M. Hyman, and J. M. Cushing, "Determining important parameters in the spread of malaria through the sensitivity analysis of a mathematical model," *Bulletin of Mathematical Biology*, vol. 70, no. 5, pp. 1272–1296, 2008.

[25] H. J. B. Njagavah and F. Nyambaza, "Modelling the impact of rehabitation amelioration and relapse on the prevalence of drug epidemics. Journal of Biology Systems," *Vol*, vol. 21, article no. 1, 2012.